Physical Layer Security in AF-Based Cooperative SWIPT Sensor Networks

Tan N. Nguyen, *Member, IEEE*, Dinh-Hieu Tran, *Student Member, IEEE*, Trinh Van Chien, *Member, IEEE*, Van-Duc Phan, Nhat-Tien Nguyen, Miroslav Voznak, *Senior Member, IEEE*, Symeon Chatzinotas, *Senior Member, IEEE*, Björn Ottersten, *Fellow, IEEE*, and H. Vincent Poor, *Life Fellow, IEEE*

***Abstract*—Physical layer security (PLS) with radio frequency (RF) energy harvesting (EH) in wireless sensor networks has received significant interest as a technology for secure information transmission and prolonging the network lifetime, as well as improving energy efficiency. This article investigates PLS for a simultaneous wireless information and power transfer (SWIPT) cooperative network, which consists of multiple sensor sources, one EH relay (R), and one destination (D) in the presence of one eavesdropper (E). Furthermore, a low-complexity, suboptimal, yet efficient sensor source selection scheme is proposed. Specifically, one sensor source is chosen to transmit information to the relay and destination such that it obtains the best channel from sensor sources to the relay. Then, by considering two relaying strategies, termed the direct link plus static power splitting-based relaying (SPSR) and direct link plus optimal dynamic power splitting-based relaying (ODPSR), the performance analysis in terms of intercept probability (IP) and outage probability (OP) is carried out for each one. Notably, the eavesdropper and destination utilize maximal ratio combining (MRC) to incorporate the received signals from the selected sensor source and the relay, which poses new challenges in obtaining the analytical expressions. In this context, we derive analytical expressions for the OP (for SPSR and ODPSR) at the destination and the IP (for SPSR) at the eavesdropper by adopting the series representation of the modified Bessel function. Finally, Monte Carlo simulations are conducted to validate the theoretical analysis and the proposed schemes' effectiveness. Simulation results show the superiority of our scheme compared to the benchmarks.**

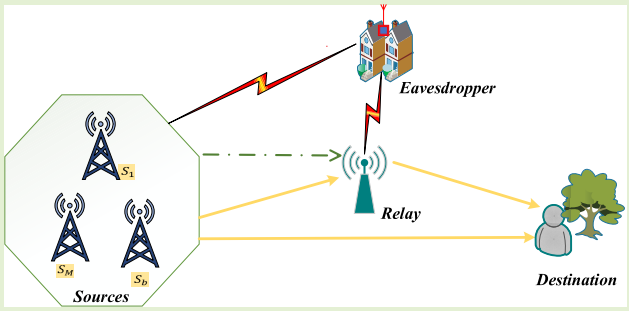

***Index Terms*— Amplify-and-forward (AF), cooperative networks, dynamic power splitting (DPS)-based relaying, energy harvesting (EH), modified Bessel functions, physical layer security (PLS), simultaneous wireless information and power transfer (SWIPT).**

I. Introduction

RECENTLY, the Internet of Things (IoT) has attracted significant attention from both industry and academia since it is a potential solution to improve the quality of life with advances such as smart cities, smart grids, health care, agriculture, and autonomous vehicles [1], [2], [3]. However, IoT users usually have limited energy capacity since they have to work remotely or operate in mobile environments. Replacing or recharging IoT devices' batteries can be costly, inconvenient, and even infeasible in harsh environments, e.g., in toxic territories or inside human bodies. Fortunately, energy harvesting (EH) has emerged as a promising solution to overcome these issues. Potential energy sensor sources include solar [4], wind, heat, and water [5], [6]. However, these natural sensor sources heavily depend on unmanageable elements, such as geographic location and weather conditions, which do not guarantee a stable energy sensor source. Therefore, radio frequency (RF) EH has attracted much attention due to its controllability and predictability [5], [6], [7].

In 2008, Varshney [8] introduced the concept of simultaneous wireless information and power transfer (SWIPT) to describe a system in which the RF signals can carry both energy and information simultaneously. Grover and Sahai [9] continued the work in [8] to a frequency-selective channel with additive white Gaussian noise (AWGN). Particularly, [9] was

Manuscript received 12 October 2022; accepted 12 November 2022. Date of publication 1 December 2022; date of current version 29 December 2022. The authors would like to thank Van Lang University, Vietnam for funding this work. The research leading to these results was supported by the Ministry of Education, Youth and Sports of the Czech Republic under the grant SP2022/5 and e-INFRA CZ (ID:90140). This research was also supported by U.S. National Science Foundation under Grant CNS-2128448. The associate editor coordinating the review of this article and approving it for publication was Prof. Pierluigi Salvo Rossi. *(Corresponding author: Van-Duc Phan.)*

Please see the Acknowledgment section of this article for the author affiliations.

Digital Object Identifier 10.1109/JSEN.2022.3224128

the first paper to investigate the information and power transfer on a coupled-inductor circuit. Different from [8] and [9], which only considered the single-input–single-output (SISO) channel model, Zhang and Ho [10], Dai et al. [11], and Pan et al. [12] investigate wireless multiple-input–multiple-output (MIMO) systems for SWIPT. In contrast to [8], [9], [10], [11], and [12] assuming a linear EH model, the nonlinear EH (NLEH) model has received significant attention from researchers recently [13], [14], [15], [16]. Raut et al. [13] studied the goodput, reliability, and energy efficiency performance of an EH-based FD IoT network for short-packet communications by considering both linear and NLEH models. Boshkovska et al. [14] aimed to maximize system throughput and fairness by jointly optimizing time allocation and power control with imperfect channel state information (CSI) and an NLEH model. To investigate the tradeoff between consumed power and harvested power, Zhang et al. [15] proposed a robust resource optimization in multi-input–single-output (MISO) cognitive radio (CR) networks under two practical NLEH models. To improve the security of CR systems, Zhou et al. [16] proposed an artificial-noise-aided cooperative jamming scheme in CR nonorthogonal multiple access (NOMA) networks with the NLEH model.

Besides the advantages of SWIPT, there remain limitations to its practical application. First, in [8] and [9], the receiver is assumed to extract power simultaneously from the same received signal, which is impractical since the circuits used for EH from RF signals cannot decode the information directly [17]. Consequently, the results in [8] and [9] only provided theoretical performance bounds. Zhang and Ho [10] proposed two practical schemes, namely, time switching (TS) and static power splitting (SPS), to coordinate the wireless information transfer (WIT) and wireless power transfer (WPT) at the receiver. Since the receivers for WIT and WPT operate at different power sensitivities, i.e., -60 and -10 dBm for information and energy, respectively [17]. Therefore, there is a tendency to optimize the WPT for a system including both WIT and WPT. This motivated Zhou et al. [17] to propose a novel system model for the SWIPT system, termed dynamic power splitting (DPS) or adaptive power splitting (APS). Therein, the received RF signals can be divided into energy and information streams with a modifiable power ratio over time. Shi et al. [18] obtained the closed-form expression of the optimal DPS ratio in a two-way DF relay network with NLEH. Apart from this, Solanki et al. [19] and Shukla et al. [20] considered the EH issues for the networks where a single transmitter sends the signals, and there are no attacks from an eavesdropper.

Due to radio communication's broadcast nature, confidential information may be intercepted/overheard by eavesdroppers. Although complexity-based cryptography can be applied to ensure secure communications, this requires complex hardware for data encryption and decryption operations and introduces extra costs for the system, such as overhead for key distribution and management [21]. Consequently, physical layer security (PLS) has emerged as a promising security provisioning solution for 5G-and-beyond networks [22], [23], [24], [25], [26], which can potentially provide secure transmissions by efficiently exploiting the characteristics of wireless channels, e.g., fading, interference, and diversity. PLS in cooperative relay networks has been widely investigated [27], [28], [29]. In cooperative relay networks, the relay nodes can play as intermediate users, applying decode-and-forward (DF), amplify-and-forward (AF), or randomized-and-forward protocols to process received signals [30], [31], [32], [33]. Tran et al. [31] proposed a generalized partial relay selection (PRS) scheme to enhance the secrecy performance of cooperative CR networks by adopting the randomize-and-forward technique with perfect and imperfect CSI from eavesdropper links. Cao et al. [34] and Arafa et al. [35] investigated secure NOMA systems in the presence of untrusted relays. Notably, Cao et al. [34] and Arafa et al. [35] proposed optimal relay selection schemes based on DF and AF protocols. Arafa et al. [36] investigated secure broadcast in a visible light communication system. Specifically, trusted cooperative relay users were introduced to support the secure transmission through multiple relaying schemes consisting of DF, AF, and cooperative jamming. Zheng et al. [37] aimed to maximize the secrecy throughput by jointly optimizing rate parameters, transmission region, and power allocation based on channel distribution information (CDI) of eavesdropping links and CSI of legitimate users. Wang et al. [38] studied a joint sensor source-relay precoding scheme that guarantees the security of an AF MIMO cooperative relay network under the presence of a multiantenna eavesdropper. In particular, Wang et al. [38] considered a direct link between a multiantenna source to a multiantenna destination and a multiantenna eavesdropper.

PLS combined with EH has recently become a promising technology to deal with secure information transmission (IT) and energy efficiency [39], [40], [41], [42]. As discussed in [40], [41], and [42], EH and cooperative jamming can be combined to improve the PLS of the system. Vo et al. [40] proposed a novel system model consisting of multiple power stations, numerous sensor nodes, one base station, and one jammer in the presence of multiple eavesdroppers. Based on the proposed model, the authors considered the enhancement of secure transmission from sensor nodes to a base station by sending jamming signals from the jammer to eavesdroppers. In [41], a secure full-duplex (FD)-relaying protocol with a jamming node was proposed to strengthen the security of data transmission from a source to a destination with the help of a friendly jammer in the presence of one eavesdropper. Cao et al. [42] proposed three EH jammer selection schemes, termed random EH jammer selection, maximal EH jammer selection, and optimal EH jammer selection, to improve the PLS for an uplink NOMA system. Ha et al. [27], Okandeji et al. [43], and Lee et al. [44] studied two-way relaying for EH PLS networks. Ha et al. [27] studied the secure transmission of a two-way half-duplex (HD) relaying network adopting PRS and hybrid time-switching and power splitting (HTPSR). Okandeji et al. [43] maximized the secrecy sum-rate by jointly optimizing the artificial noise covariance matrix, transmit power, and beamforming for an SWIPT system with an FD AF relay. Lee et al. [44] considered a secure two-way relay network that uses EH in the presence of a multieavesdropper. They proposed two schemes,

termed TS-based two-way relaying and power splitting-based two-way relaying, to maximize the minimum ensured secrecy capacity.

Despite significant achievements in the above works, there is still a need for research on PLS and SWIPT in cooperative relay networks. Specifically, due to their complexity, analytical expressions for outage probability (OP) and intercept probability (IP) are challenging to obtain. Lee et al. [45] studied a simple model with a source, an AF relay, and a destination. However, Lee et al. [45] only achieved a simplified OP expression based on a high signal-to-noise ratio (SNR) approximation. Another example is that Ye et al. [46] instigated the outage performance for a DF relay network with one source, one DF relay, and one destination. Nevertheless, the OP expression was derived using the Gaussian–Chebyshev quadrature with a higher gap between simulation and mathematical results. In the performance analysis of secure cooperative networks, maximal ratio combining (MRC) introduces difficulties in deriving the OP and IP compared with maximal ratio transmission (MRT) because the destination/eavesdropper can combine signals from multiple sources in the former case.

Although the security performance factors, such as secrecy capacity or secrecy OP (SOP), are used more popularly to investigate the PLS models, in some special situations, the analysis of the tradeoff between the security performance (in terms of IP) and the reliability performance (in terms of OP) is more suitable [47], [48], [49]. In particular, our proposed OP and IP analysis can be applied to the wireless relay networks that cannot be supported by security enhancement methods at the physical layer due to low cost or simple circuitry and only need moderate security requirements. Due to the lack of security enhancement techniques, the secrecy capacity and SOP are not good, and analyzing these performance factors does not help much. In contrast, IP and OP analyses help assess the tradeoff in reliability and security so that the designer can decide whether to configure parameters that meet the OP and IP requirements.

In this article, we present an AF-based SWIPT sensor network for secure communications in the presence of an eavesdropper. Moreover, the direct link is taken into account to improve the performance at the destination. The eavesdropper and destination adopt MRC to combine the chosen sensor source and relay information. The main contributions of this research are summarized as follows.

1) To the best of our knowledge, this is the first work that applies the series representations for the modified Bessel function to obtain analytical expressions for the OP and IP in AF-based SWIPT cooperative networks with a direct link. Specifically, we provide analytical expressions for the OP of both SPS-based relaying (SPSR) and optimal dynamic PS-based relaying (ODPSR), and the IP for SPSR by adopting the series representation of modified Bessel functions. This is especially challenging since the probability analysis involves many random variables (RVs), and the MRC is enabled at the eavesdropper and destination, making the derivation more complicated. The simulation results confirmed that our derived analytical expression for OP and IP matches well with the exact ones, i.e., numerical results. Particularly, it shows that the gap between simulation and mathematical expression in our work is much better than the benchmarks [45], [46].
2) We conduct a mathematical analysis of the optimal value of the power splitting factor ρ to maximize the transmission rate at the destination, i.e., C_D. To this end, we prove that the destination's rate expression is a concave function. The candidates for the optimal value of ρ, denoted by $\rho^\star$, are achieved by taking the first derivative of C_D and equating it to zero. $\rho^\star$ is, finally, obtained by excluding other unreasonable cases. Notably, $\rho^\star$ can be found before the beginning of data transmission.
3) Monte Carlo simulations are performed to verify the correctness of our analysis. The simulations also provide an insightful analysis of the tradeoff between the OP and IP of the proposed SPSR and ODPSR schemes.

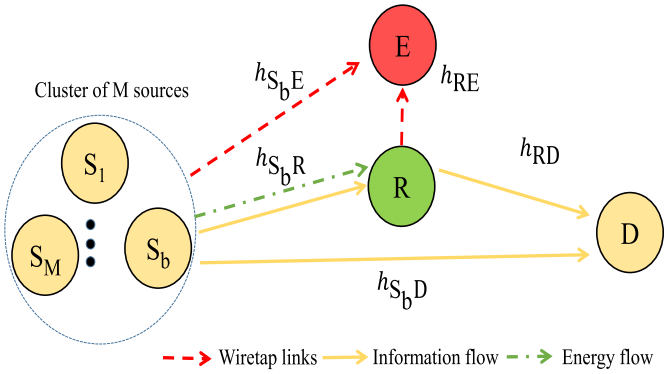

Fig. 1. Considered system model.

The rest of this article is organized as follows. Section II describes the proposed system model. Then, the derivation of key performance metrics, including the OP and IP of the proposed model, is presented in Section III. Section IV presents the numerical results obtained from both analysis and Monte Carlo simulations. Finally, Section V concludes this article.

II. System Model

We consider a cooperative relaying network, as shown in Fig. 1, with multiple sensor sources, denoted by $\mathcal{S} \triangleq \{S_1, \ldots, S_b, \ldots, S_M\}$, one relay R, and one destination D in the presence of one eavesdropper E. Specifically, an eavesdropper is trying to overhear the information transmitted from the sensor source and relay by applying the MRC technique. Moreover, the direct link from $S_b \rightarrow D$ is considered to enhance the performance at the destination. We assume that the multiple sensor source nodes are located in a cluster, which means that the distances from every available sensor source node to a relay and eavesdropper node are approximately identical. This assumption is reasonable in practice, especially for IoT device networks or wireless sensor networks. Besides, the sensor sources, relay, destination, and eavesdropper are single-antenna devices and operate in the HD mode. In Fig. 2, the relay node is equipped with an energy harvester that can

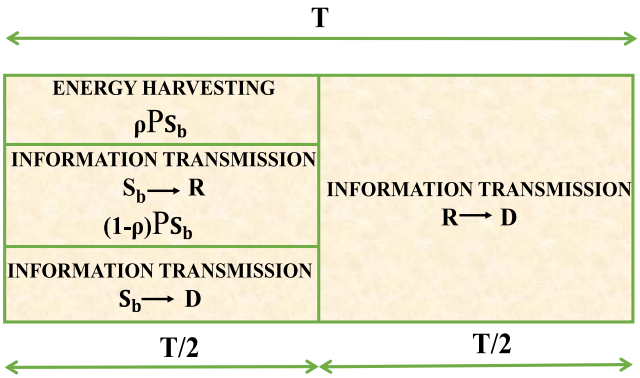

Fig. 2. Schematic illustration of EH and IT processes with a power splitting relaying protocol at the relay.

harvest energy from the best sensor source S_b by utilizing the power splitting method. Specifically, a power divider is used to split the received signals into two portions: a fraction of power ρP is used for EH, and the second part $(1-\rho)P$ is used for data transmission, whereas $\rho \in [0, 1]$ is the power splitting factor, with ρ equal to zero (or one) meaning that total received signals are used for EH (or information transfer). Next, the IT process from R to D is conducted in the remaining half-time duration $T/2$ [50], [51], [52].

Assume that the channels between two arbitrary nodes are block Rayleigh-fading, where channel coefficients remain constant during one transmission block and change independently across different transmission blocks.[1] Thus, the squared amplitudes of the channel gains, such as $|h_{\mathrm{RE}}|^2$, $|h_{\mathrm{RD}}|^2$, are exponential RVs whose cumulative distribution function (CDF) and probability density function (pdf) have the following forms, respectively:

$$F_Z(z) = 1 - e^{-\lambda z} \tag{1}$$

$$f_Z(z) = \begin{cases} \lambda e^{-\lambda z}, & \text{if } z \geq 0 \\ 0, & \text{if } z < 0 \end{cases} \tag{2}$$

where λ is the rate parameter of the exponential RV Z. This article assumes that the CSI is available at the relay, the destination, and even as the eavesdropper. It should be noted that it is more convenient for the relay/destination than the eavesdropper to estimate the CSI of the channel from the sensor source because they are cooperative. However, in practical consideration, the eavesdropper can obtain the CSI from the sensor source. For example, the eavesdropper can use blind channel estimation techniques [54], [55]. In our analysis, it should be more reasonable that we should consider the worst case for our analysis, i.e., perfect CSI at the eavesdropper.

Next, we present the mathematical analysis for the entire process. As mentioned above, suppose that sensor source S_b is chosen to send information and energy to the relay R. During the first transmission phase, the received signal at the relay can be given by

$$y_R = \sqrt{(1-\rho)} h_{S_b R} x_{S_b} + n_R \tag{3}$$

where $b \in (1, 2, \ldots, M)$; x_{S_b} is the transmitted signal at the bth sensor source; n_R is the AWGN with variance N_0; and $\mathbb{E}\{|x_{S_b}|^2\} = P_{S_b}$, where $\mathbb{E}\{\cdot\}$ is the expectation operator, and P_{S_b} is the average transmit power at the bth sensor source. By adopting the power splitting technique, the relay's transmit power can be obtained as

$$\begin{aligned} P_R &= \frac{E_h}{T/2} = \frac{\eta\rho P_{S_b} \left|h_{S_b R}\right|^2 (T/2)}{T/2} \\ &= \eta\rho P_{S_b} \left|h_{S_b R}\right|^2 \end{aligned} \tag{4}$$

where E_h is the received energy at the relay; T is the coherence time; and $0 < \eta \leq 1$ is energy conversion efficiency, which considers the energy loss due to harvesting, decoding, and processing circuits. Next, the received signal at the destination (D) from the sensor source (in the first phase) and relay (in the second phase) can be, respectively, expressed as

$$\begin{aligned} y_D^1 &= h_{S_b D} x_{S_b} + n_D^1 \\ y_D^2 &= h_{RD} x_R + n_D^2 \end{aligned} \tag{5}$$

where $n_D^2 = n_D^1 = n_D$ is AWGN with variance N_0; the transmitted signal from relay, denoted by x_R, satisfies $\mathbb{E}\{|x_R|^2\} = P_R$; and $b \in (1, \ldots, M)$. Since the eavesdropper can overhear the information from both the sensor source and relay nodes, the received signals at E in the first and second phases are, respectively, given by

$$\begin{aligned} y_E^1 &= h_{S_b E} x_{S_b} + n_E^1 \\ y_E^2 &= h_{RE} x_R + n_E^2 \end{aligned} \tag{6}$$

where we assume that $n_E^1 = n_E^2 = n_E$ is the AWGN with variance N_0 and $b \in (1, \ldots, M)$. In our proposed system, we consider the AF technique. Therefore, the signal transmitted by the relay is an amplified version of y_R, which is denoted by a factor β

$$\beta = \frac{x_R}{y_R} = \sqrt{\frac{P_R}{(1-\rho) P_{S_b} \left|h_{S_b R}\right|^2 + N_0}}. \tag{7}$$

From (3) and (5), the received signal at D in the second phase can be rewritten by

$$\begin{aligned} y_D^2 &= h_{\mathrm{RD}} \beta y_R + n_D \\ &= h_{\mathrm{RD}} \beta \left[\sqrt{(1-\rho)} h_{S_b R} x_{S_b} + n_R\right] + n_D \\ &= \underbrace{\sqrt{(1-\rho)} h_{S_b R} x_{S_b} h_{RD} \beta}_{signal} + \underbrace{h_{RD} \beta n_R + n_D}_{noise}. \end{aligned} \tag{8}$$

Hence, the SNR at D in this phase can be obtained as follows:

$$\begin{aligned} \gamma_D^2 &= \frac{E\left\{|\text{signal}|^2\right\}}{E\left\{|\text{noise}|^2\right\}} = \frac{(1-\rho) P_{S_b} \left|h_{S_b R}\right|^2 |h_{\mathrm{RD}}|^2 \beta^2}{|h_{\mathrm{RD}}|^2 \beta^2 N_0 + N_0} \\ &= \frac{(1-\rho) P_{S_b} \left|h_{S_b R}\right|^2 |h_{\mathrm{RD}}|^2}{|h_{\mathrm{RD}}|^2 N_0 + \frac{N_0}{\beta^2}}. \end{aligned} \tag{9}$$

[1] Due to the complex propagation environments, the relay and destination may be blocked due to large obstacles. Consequently, the propagation channels with the NLoS components should be applicable to these practical scenarios. Rayleigh fading channels are popularly utilized for rich scattering conditions, such as dense urban areas [53]. In this article, we have demonstrated that the relay can still harvest sufficient energy to amplify and forward the information.

After doing some algebraic manipulations and due to the fact that $N_0 << P_R$, we have

$$\gamma_D^2 = \frac{(1-\rho)\, P_{S_b} P_R \left|h_{S_b R}\right|^2 |h_{\mathrm{RD}}|^2}{|h_{\mathrm{RD}}|^2 P_R N_0 + (1-\rho)\, P_{S_b} \left|h_{S_b R}\right|^2 N_0}. \tag{10}$$

By combining with (4), the SNR γ_D^2 can be expressed as

$$\gamma_D^2 = \frac{\eta\rho\,(1-\rho)\,\Psi \left|h_{S_b R}\right|^2 |h_{RD}|^2}{\eta\rho |h_{RD}|^2 + (1-\rho)} \tag{11}$$

where $\Psi = P_{S_b}/N_0$. Furthermore, D also receives direct signals from the selected sensor source during the first phase. Therefore, the corresponding SNR can be computed as

$$\gamma_D^1 = \Psi \left|h_{S_b D}\right|^2. \tag{12}$$

Since D adopts the MRC to incorporate the information from the sensor source and relay nodes, consequently, the overall SNR at D can be given by

$$\gamma_D = \gamma_D^1 + \gamma_D^2 = \frac{\eta\rho\,(1-\rho)\,\Psi \left|h_{S_b R}\right|^2 |h_{\mathrm{RD}}|^2}{\eta\rho |h_{\mathrm{RD}}|^2 + (1-\rho)} + \Psi \left|h_{S_b D}\right|^2. \tag{13}$$

We assume that the eavesdropper also adopts MRC, and its SNR can be expressed as

$$\gamma_E = \frac{\eta\rho\,(1-\rho)\,\Psi \left|h_{S_b R}\right|^2 |h_{\mathrm{RE}}|^2}{\eta\rho |h_{\mathrm{RE}}|^2 + (1-\rho)} + \Psi \left|h_{S_b E}\right|^2. \tag{14}$$

Remark 1: From a practical point of view, we may reasonably assume that the sensor source selector has no knowledge of the instantaneous CSI from the relay to the destination but has knowledge of CSI from sensor sources to the relay. Therefore, we propose a suboptimal sensor source selection protocol in which the best is selected as follows.[2]

$$b = \arg \max_{1 \le b \le M} \left|h_{S_b R}\right|^2. \tag{15}$$

It should be noted that the sensor source selection algorithm does not change the nature of the channel distributions of the sensor source-to-destination/eavesdropper links because the sensor source-to-destination/eavesdropper links do not depend on the sensor source-to-relay channel gain. The pdf of the sensor source-to-destination/eavesdropper link can be represented as

$$f_{S_b X}(x) = \begin{cases} \lambda_{S_b X} e^{-\lambda_{S_b X} x}, & \text{if } x > 0 \\ 0, & \text{otherwise} \end{cases} \tag{16}$$

where $X \in \{D, E\}$. By denoting $\omega_1 = \max_{b=1,2,\ldots,M}(|h_{S_b R}|^2)$, the CDF of ω_1 can be given by [27]

$$F_{\omega_1}(x) = \sum_{n=0}^{M} (-1)^n C_M^n e^{-\lambda_1 n x} = 1 + \sum_{n=1}^{M} (-1)^n C_M^n e^{-\lambda_1 n x} \tag{17}$$

[2]Previous works, such as [56], share a commonality with us but with a vast difference. In particular, Salem et al. [56] consider the data transmission from a given sensor source, while we are selecting the best candidate among multiple sensors. This distinction leads to new analytical results. Furthermore, the OP and IP are the measurement metrics in this article instead of the ergodic secrecy capacity [56]

where $C_M^n = (M!/n!(M-n)!)$ and λ_1 is the mean of RV ω_1. Then, the corresponding pdf can be represented as

$$f_{\omega_1}(x) = \lambda_1 \sum_{n=0}^{M-1} (-1)^n C_{M-1}^n M \times e^{-\lambda_1 (n+1) x}. \tag{18}$$

Without loss of generality, we assume that total time T is set to the unit value. Thus, the data transmission rate (bps/Hz) at E and D are, respectively, expressed as follows:

$$\begin{aligned} C_E &= \log_2(1+\gamma_E) \\ C_D &= \log_2(1+\gamma_D) \end{aligned} \tag{19}$$

which rely on the complete availability of the instantaneous CSI that can be estimated numerically over many different realizations of small scale-fading coefficients. A numerical evaluation based on (19) has a high computational complexity, motivating us to work on the performance analysis with statistical CSI only hereafter.

Remark 2: The coexistence of the sensor selection and the eavesdropper, together with a direct link from the selected sensor to the destination, creates new contributions to this article. By choosing the sensor with the best channel gain among a cluster of M sensors, we establish an initial framework on the PLS for relay cooperative SWIPT sensor networks and obtain the analytical results of the outage and IP. Extended directions, including multiple relays, eavesdroppers, and destinations, should be interesting for future work.

III. Performance Analysis

This section provides the mathematical analysis of the OP and IP to provide further insight into the end-to-end transmission for AF-based SWIPT relay networks.

A. Outage Probability

From the definition of data transmission rate in (19), the OP of the system can be defined as

$$\mathrm{OP} = \Pr(C_D < C_{\mathrm{th}}) \tag{20}$$

where C_{th} is a predetermined target rate.

1) Static Power Splitting-Based Relaying: In this scenario, the power splitting ratio ρ value is kept at a fixed value. By combining (13) and (19), the OP can be rewritten as

$$\begin{aligned} \mathrm{OP}^{\mathrm{SPSR}} &= \Pr(\gamma_D < \gamma_{th}) \\ &= \Pr\left(\frac{\eta\rho\,(1-\rho)\,\Psi \max\left(\left|h_{S_b R}\right|^2\right) |h_{RD}|^2}{\eta\rho |h_{\mathrm{RD}}|^2 + (1-\rho)} \right. \\ &\qquad \left. + \Psi |h_{S_j D}|^2 < \gamma_{th} \right) \\ &= \Pr(X + Y < \gamma_{th}) \\ &= \int_0^{\gamma_{th}} F_X(\gamma_{th} - y | Y = y)\, f_Y(y)\, dy \\ &= \int_0^{\gamma_{th}} F_X(x)\, f_Y(\gamma_{th} - x)\, dx \end{aligned} \tag{21}$$

where $\gamma_{th} = 2^{C_{th}} - 1$, $X = (\eta\rho(1-\rho)\Psi \times \max(|h_{S_b R}|^2)|h_{\mathrm{RD}}|^2)/(\eta\rho|h_{\mathrm{RD}}|^2 + (1-\rho))$, and $Y = \Psi \times |h_{S_b D}|^2$.

Lemma 1: The CDF function of X can be given as

$$F_X(x) = 1 + 2\sum_{n=1}^{M}(-1)^n C_M^n \exp\left(-\frac{\lambda_1 n x}{(1-\rho)\Psi}\right) \times \sqrt{\frac{\lambda_1\tilde{\lambda}_1 n x}{\eta\rho\Psi}} \times K_1\left[2\sqrt{\frac{\lambda_1\tilde{\lambda}_1 n x}{\eta\rho\Psi}}\right] \quad (22)$$

where $\tilde{\lambda}_1$ is the mean of RV φ_1 and $K_v\{\cdot\}$ is the modified Bessel function of second kind with the vth order.

Proof: See Appendix A. ∎

Next, the CDF and pdf of Y can be, respectively, expressed as

$$F_Y(y) = \Pr(Y < y) = \Pr\left(\Psi \times |h_{S_bD}|^2 < y\right) = \Pr\left(\omega_2 < \frac{y}{\Psi}\right) = 1 - \exp\left(-\frac{\lambda_2 y}{\Psi}\right) \quad (23)$$

$$f_Y(y) = \frac{\partial F_Y(y)}{\partial y} = \frac{\lambda_2}{\Psi}\exp\left(-\frac{\lambda_2 y}{\Psi}\right). \quad (24)$$

By substituting (22) and (24) into (21), the OP can be given by (25), as shown at the bottom of the page.

Remark 3: Notably, the integration shown in the last term of (25) has no closed-form result to the best of our knowledge. Many authors also tried to find the exact analytical expression in previous works and presented this problem in [57] and [58] when applying the MRC at the receiver. However, their mathematical expressions show a lower exactness than our proposed method. In contrast to the aforementioned works, this article can derive the analytical solution using a series representation of modified Bessel functions.

Lemma 2: In an SPS relaying system, the analytical expression of OP at the destination D can be described by (26), as shown at the bottom of the page.

Proof: See Appendix B. ∎

2) Optimal Dynamic Power Splitting-Based Relaying: In this scenario, we try to find the optimal $\rho^\star$ value to maximize the capacity C_D. By observing (19), we have $\max(C_D) \Leftrightarrow \max(\gamma_D)$. It is easy to prove that $(\partial^2\gamma_D/\partial\rho^2)$ is negative for all $0 < \rho < 1$. Hence, we conclude that γ_D is a concave function of ρ. We can find the value of ρ to maximize γ_D by differentiating γ_D concerning ρ and then equate it to zero. After doing some algebraic calculations, $\rho^\star$ can be expressed as $\rho^\star = (1/1 + |h_{\mathrm{RD}}|(\eta)^{1/2})$ or $\rho^* = (1/1 - |h_{\mathrm{RD}}|(\eta)^{1/2})$. Since $\rho^\star = (1/1 - |h_{\mathrm{RD}}|(\eta)^{1/2})$ results in a value of $\rho^\star > 1$ or $\rho^\star < 0$, $\rho^\star = (1/1 + |h_{\mathrm{RD}}|(\eta)^{1/2})$ is selected as the optimal solution. Substituting this optimal $\rho^\star$ into (21), the OP is computed by

$$\mathrm{OP}^{\mathrm{ODPSR}} = \Pr\left(\frac{\eta\Psi\omega_1\varphi_1}{\left(1+\sqrt{\eta\varphi_1}\right)^2} + \Psi\omega_2 < \gamma_{th}\right) \quad (27)$$

where $\varphi_1 \triangleq |h_{\mathrm{RD}}|^2$, $\omega_1 \triangleq \max_{b=1,2,\ldots,M}(|h_{S_bR}|^2)$, and $\omega_2 \triangleq |h_{S_bD}|^2$. Moreover, (27) can be rewritten as

$$\begin{aligned}\mathrm{OP}^{\mathrm{ODPSR}} &= \Pr\left(\widetilde{X} + \widetilde{Y} < \gamma_{th}\right) \\ &= \int_0^{\gamma_{th}} F_{\widetilde{X}}(\gamma_{th} - \widetilde{y}) \times f_{\widetilde{Y}}(\widetilde{y})\, d\widetilde{y} \\ &= \int_0^{\gamma_{th}} F_{\widetilde{X}}(\widetilde{x}) \times f_{\widetilde{Y}}(\gamma_{th} - \widetilde{x})\, d\widetilde{x} \end{aligned} \quad (28)$$

where $\widetilde{X} \triangleq (\eta\Psi\omega_1\varphi_1/(1+(\eta\varphi_1)^{1/2})^2)$ and $\widetilde{Y} \triangleq \Psi\omega_2$.

Lemma 3: The closed-form expression of $F_{\widetilde{X}}$ is given by

$$\begin{aligned} F_{\widetilde{X}}(\widetilde{x}) &= 1 + 2\sum_{k=0}^{\infty}\sum_{n=1}^{M}\frac{(-1)^{k+n}C_M^n(2\lambda_1 n\widetilde{x})^k\tilde{\lambda}_1}{\Psi^k\eta^{k/2}k!}\exp\left(-\frac{\lambda_1 n\widetilde{x}}{\Psi}\right) \times\left(\frac{\lambda_1 n\widetilde{x}}{\eta\Psi\tilde{\lambda}_1}\right)^{(-0.25\ k+0.5)} K_{-k/2+1}\left(2\sqrt{\frac{\lambda_1\tilde{\lambda}_1 n\widetilde{x}}{\eta\Psi}}\right) \\ &= 1 + \sum_{k=0}^{\infty}\sum_{n=0}^{M}\frac{(-1)^{k+n}2^{k+1}C_M^n}{k!}\left(\frac{\tilde{\lambda}_1}{\eta}\right)^{\frac{k}{4}+0.5}\left(\frac{\lambda_1 n\widetilde{x}}{\Psi}\right)^{\frac{3k}{4}+0.5} \times\exp\left(-\frac{\lambda_1 n\widetilde{x}}{\Psi}\right)\times K_{-k/2+1}\left(2\sqrt{\frac{\lambda_1\tilde{\lambda}_1 n\widetilde{x}}{\eta\Psi}}\right) \end{aligned} \quad (29)$$

$$\mathrm{OP}^{\mathrm{SPSR}} = 1 - \exp\left(-\frac{\lambda_2\gamma_{th}}{\Psi}\right) + 2\sum_{n=1}^{M}\frac{(-1)^n C_M^n\lambda_2}{\Psi}\times\exp\left(-\frac{\lambda_2\gamma_{th}}{\Psi}\right) \times \underbrace{\int_0^{\gamma_{th}}\exp\left(\frac{\lambda_2 x}{\Psi} - \frac{\lambda_1 n x}{(1-\rho)\Psi}\right)\times\sqrt{\frac{\lambda_1\tilde{\lambda}_1 n x}{\eta\rho\Psi}}\times K_1\left[2\sqrt{\frac{\lambda_1\tilde{\lambda}_1 n x}{\eta\rho\Psi}}\right]dx}_{\Xi} \quad (25)$$

$$\begin{aligned}\mathrm{OP}^{\mathrm{SPSR}} &= 1 - \exp\left(-\frac{\lambda_2\gamma_{th}}{\Psi}\right) + \widetilde{\sum}\frac{(-1)^{n+t}(2)^{2i-1+t}\Lambda(1,l,i)\,C_M^n\lambda_2}{t!\Psi}\times\exp\left(-\frac{\lambda_2\gamma_{th}}{\Psi}\right) \\ &\times\left[\frac{\lambda_1\tilde{\lambda}_1 n}{\eta\rho\Psi}\right]^{\frac{i+t}{2}}\times\left[\frac{\lambda_1 n}{(1-\rho)\Psi} - \frac{\lambda_2}{\Psi}\right]^{\left(-\frac{i+t+2}{2}\right)}\times\gamma\left(\frac{i+t+2}{2}, \left[\frac{\lambda_1 n}{(1-\rho)\Psi} - \frac{\lambda_2}{\Psi}\right]\times\gamma_{th}\right) \end{aligned}$$

$$\text{where } \widetilde{\sum} = \sum_{t=0}^{\infty}\sum_{l=0}^{\infty}\sum_{i=0}^{l}\sum_{n=1}^{M} \quad (26)$$

where $K_1(\cdot)$ is the modified Bessel function of the second kind and 1-order. In particular, $K_1(2((\lambda_1\tilde{\lambda}_1 nx/\eta\rho\Psi))^{1/2})$ can be rewritten as follows:

$$K_1\left(2\sqrt{\frac{\lambda_1\tilde{\lambda}_1 nx}{\eta\rho\Psi}}\right)=\sum_{t=0}^{\infty}\sum_{l=0}^{\infty}\sum_{i=0}^{l}\left[\frac{\lambda_1\tilde{\lambda}_1 n}{\eta\rho\Psi}\right]^{\frac{i-1+t}{2}} \times\frac{(-1)^t(2)^{2i-2+t}}{t!}\Lambda(1,l,i)\,x^{\frac{i-1+t}{2}}. \quad (30)$$

Proof: See Appendix C. ∎

Based on (24) and (29), the expression of $\mathrm{OP}^{\mathrm{ODPSR}}$ can be expressed as in (31), shown at the bottom of the page.

Remark 4: In (31), there still exists an integral in the OP expression. Thus, we need to perform some mathematical manipulation to remove the integral.

Theorem 1: In the DPS relaying system, the analytical expression of OP at the destination D can be expressed as

$$\begin{aligned}\mathrm{OP}^{\mathrm{ODPSR}} &= 1-\exp\left(-\frac{\lambda_2\gamma_{th}}{\Psi}\right)+\widetilde{\sum}^{*}\frac{(-1)^{\zeta_1}2^{\zeta_2}C_M^n\lambda_2\Lambda(q,l,i)}{k!t!}\\ &\times\left(\frac{\tilde{\lambda}_1}{\eta}\right)^{\zeta_3}\left(\frac{\lambda_1 n}{\Psi}\right)^{\zeta_4}\exp\left(-\frac{\lambda_2\gamma_{th}}{\Psi}\right)\\ &\times\left[\frac{\lambda_1 n}{\Psi}-\frac{\lambda_2}{\Psi}\right]^{-\zeta_5}\gamma\left[\zeta_5,\left(\frac{\lambda_1 n}{\Psi}-\frac{\lambda_2}{\Psi}\right)\gamma_{th}\right] \quad (32)\end{aligned}$$

where $\zeta_1 \triangleq k+n+t$, $\zeta_2 \triangleq 2i+2k+t-1$, $\zeta_3 \triangleq 0.5(k+i+t)$, $\zeta_4 \triangleq 0.5(2k+i+t)$, and $\zeta_5 \triangleq 0.5(i+t+2k+2)$.

Proof: See Appendix D. ∎

The OPs in (26) and (32) are upper bounded by one and include the effects of the eavesdropper and the relay selection. We note that the SOP is nontrivial to obtain and should be a potential topic for further work.

B. Intercept Probability

The considered system will be wiretapped if E can successfully decode received signals from the sensor source and relay [24], i.e., $C_E \geq C_{th}$. Therefore, the IP of the system can be expressed by

$$\mathrm{IP}=\Pr(C_E\geq C_{th})=1-\Pr(C_E<C_{th}). \quad (33)$$

1) Static Power Splitting-Based Relaying:

Theorem 2: In an SPS relaying system, the analytical expression of IP at E can be given by

$$\mathrm{IP}^{\mathrm{SPSR}}=\exp\left(-\frac{\lambda_3\gamma_{th}}{\Psi}\right)-\widetilde{\sum}\frac{(-1)^{\zeta_6}(2)^{\zeta_7}\Lambda(1,l,i)\,C_M^n\lambda_3}{t!\Psi} \times\exp\left(-\frac{\lambda_3\gamma_{th}}{\Psi}\right)\left[\frac{\lambda_1\tilde{\lambda}_2 n}{\eta\rho\Psi}\right]^{\zeta_8}\left[\frac{\lambda_1 n}{(1-\rho)\Psi}-\frac{\lambda_3}{\Psi}\right]^{-\zeta_9} \times\gamma\left(\zeta_9,\left[\frac{\lambda_1 n}{(1-\rho)\Psi}-\frac{\lambda_3}{\Psi}\right]\gamma_{th}\right) \quad (34)$$

where $\tilde{\lambda}_2$ and λ_3, respectively, denote the mean of RVs $|h_{\mathrm{RE}}|^2$ and $|h_{S_bE}|^2$; $\zeta_6 \triangleq n+t$, $\zeta_7 \triangleq 2i-1+t$, $\zeta_8 \triangleq 0.5(i+t)$, and $\zeta_9 \triangleq 0.5(i+t+2)$.

Proof: We can obtain the proof for (34) as the same as the proof for (26), which is shown in Appendix B. ∎

2) Optimal Dynamic Power Splitting-Based Relaying:

By substituting optimal power splitting ratio $\rho^* = (1/1+|h_{\mathrm{RD}}|(\eta)^{1/2})$ into (14), the SNR at E can be written by

$$\gamma_E^{\mathrm{ODPSR}}=\frac{\frac{\eta\tilde{\varphi}_1}{1+\tilde{\varphi}_1}\Psi\omega_1\varphi_2}{\eta\varphi_2+\tilde{\varphi}_1}+\Psi\omega_3 \quad (35)$$

where $\tilde{\varphi}_1 = (\eta|h_{\mathrm{RD}}|^2)^{1/2} = (\eta\varphi_1)^{1/2}$, $\omega_1 = \max_{b=1,2,\ldots,M}(|h_{S_bR}|^2)$, $\varphi_2 = |h_{\mathrm{RE}}|^2$, and $\omega_3 = |h_{S_bE}|^2$.

Then, $\mathrm{IP}^{\mathrm{ODPSR}}$ can be expressed as

$$\begin{aligned}\mathrm{IP}^{\mathrm{ODPSR}} &= 1-\Pr(T+Z<\gamma_{th})\\ &= 1-\int_0^{\gamma_{th}}F_T(\gamma_{th}-z)\,f_Z(z)\,dz\\ &= 1-\int_0^{\gamma_{th}}F_T(t)\,f_Z(\gamma_{th}-t)\,dt \quad (36)\end{aligned}$$

where $T=((\eta\tilde{\varphi}_1/1+\tilde{\varphi}_1)\Psi\omega_1\varphi_2/\eta\varphi_2+\tilde{\varphi}_1)$ and $Z=\Psi\omega_3$. To obtain $\mathrm{IP}^{\mathrm{ODPSR}}$, we first need to find the $F_T(t)$ expression, which is given as the following lemma.

Lemma 4: The CDF of T, i.e., $F_T(t)$, can be expressed as follows:

$$\begin{aligned}F_T(t) &= 1+2\sum_{r=0}^{\infty}\sum_{s=0}^{\infty}\sum_{n=1}^{M}\frac{(-1)^{n+s+r}C_M^n\exp\left(-\frac{\lambda_1 nt}{\Psi}\right)}{r!s!}\\ &\times\left(\frac{\lambda_1 nt}{\Psi}\right)^{s}\left(\frac{\tilde{\lambda}_1}{\eta}\right)^{r+1}\Gamma(2r-s+2)\\ &\times G_{1,3}^{3,0}\left(\frac{4\lambda_1\tilde{\lambda}_2 nt}{\eta\Psi}\middle|\begin{matrix}0\\-2r+s-2,1,0\end{matrix}\right) \quad (37)\end{aligned}$$

where $\Gamma(\cdot)$ is the gamma function and $G_{p,q}^{m,n}(z|\begin{matrix}a_1,\ldots,a_p\\b_1,\ldots,b_q\end{matrix})$ is the Meijer G-function.

Theorem 3: In the optimal DPS relaying system, $\mathrm{IP}^{\mathrm{ODPSR}}$ at E can be calculated as

$$\mathrm{IP}^{\mathrm{ODPSR}}=\exp\left(-\frac{\lambda_3\gamma_{th}}{\Psi}\right)-\widetilde{\sum}^{**}\int_0^{\gamma_{th}}\Delta(t)\,dt \quad (38)$$

$$\mathrm{OP}^{\mathrm{ODPSR}}=1-\exp\left(-\frac{\lambda_2\gamma_{th}}{\Psi}\right)+\sum_{k=0}^{\infty}\sum_{n=1}^{M}\frac{(-1)^{k+n}2^{k+1}C_M^n\lambda_2}{k!\Psi}\times\left(\frac{\tilde{\lambda}_1}{\eta}\right)^{k/4+1/2}\times\left(\frac{\lambda_1 n}{\Psi}\right)^{3k/4+1/2} \times\exp\left(-\frac{\lambda_2\gamma_{th}}{\Psi}\right)\times\int_0^{\gamma_{th}}\tilde{x}^{3k/4+1/2}\times\exp\left[\frac{\lambda_2\tilde{x}}{\Psi}-\frac{\lambda_1 n\tilde{x}}{\Psi}\right]\times K_{-k/2+1}\left(2\sqrt{\frac{\lambda_1\tilde{\lambda}_1 n\tilde{x}}{\eta\Psi}}\right)d\tilde{x} \quad (31)$$

where the following definition holds:

$$\widetilde{\sum}^{**} = \sum_{r=0}^{\infty}\sum_{s=0}^{\infty}\sum_{n=1}^{M} \tag{39}$$
$$\Delta(t)$$
$$= \frac{(-1)^{n+s+r} C_M^n \times \Gamma(2r-s+2) \times \exp\left(\frac{\lambda_3 t}{\Psi} - \frac{\lambda_1 nt}{\Psi}\right)}{r!s!}$$
$$\times \left(\frac{\lambda_1 nt}{\Psi}\right)^s \left(\frac{\tilde{\lambda}_1}{\eta}\right)^{r+1} G_{1,3}^{3,0}$$
$$\times \left(\frac{4\lambda_1\tilde{\lambda}_2 nt}{\eta\Psi}\middle| \begin{matrix} 0 \\ -2r+s-2, 1, 0 \end{matrix}\right). \tag{40}$$

Proof: By substituting (37) into (36), we can obtain (38), which finishes the proof. ■

Remark 5: Similar to the observations for the OP, the IP is upper bounded by one and contains the effects of the transmit power from the relay and the attacks from the eavesdropper. We stress that the adopted definition of the IP does not explicitly take into account the legitimate link. Nonetheless, by direct inspection of the signal-to-noise-and-interference ratio (SINR) of γ_E, one can observe that both indirect links at the legitimate and eavesdropper go through the relay. As a result, if the first hop from S $\rightarrow$ R is wiretapped, the information bound for D will eavesdrop, and the considered IP is consistently taken into consideration the secrecy of the considered networks. As demonstrated by many previous works in the literature [24], [59], the IP has been considered an important metric when studying the security issue at the physical layer.

Remark 6: The obtained analytical results are independent of small-scale fading coefficients, which work for a long period of time and reduce the computational complexity of evaluating the OP and IP. We emphasize the asymptotic analysis of interest in observing system performance in the limiting regimes. However, obtaining the analytical results for the OP and IP is nontrivial as it increases the network dimensions due to the intricacies of computing and analyzing the modified Bessel function. This potential analysis is left for future work.

IV. Simulation Results

In this section, Monte Carlo simulations are provided to validate the theoretical expressions and the impacts of various parameters on the system performance. To obtain the IP and OP for the proposed schemes, we perform 10^6 independent trials, and the channel coefficients are randomly generated as Rayleigh fading in each trial. The settings of simulation parameters are listed in Table I. Unless otherwise stated, we assumed that the predetermined target rate is set as $C_{\text{th}} = 0.5$ bps/Hz, the energy conversion efficiency $\eta = 0.8$, the SPS ratio $\rho = 0.8$, $\Psi = -5$ dB, and the total number of sensor sources $M = 2$ [60]. In the simulation environment, let us consider a linear topology in which the distances of the links $S_b \rightarrow R$, $R \rightarrow D$, $S_b \rightarrow D$, $S_b \rightarrow E$, and $R \rightarrow E$ are, respectively, set as $d_{S_bR} = 0.5$, $d_{\text{RD}} = 0.5$, $d_{S_bD} = 1$, $d_{S_bE} = 2$, and $d_{\text{RE}} = 1.5$ [59]. Besides, we adopt a simplified path loss model, i.e., $\lambda_U = d_U^{\alpha}$, with $U \in \{d_{S_bR}, d_{\text{RD}}, d_{S_bD}, d_{S_bE}, d_{\text{RE}}\}$, and α is the path-loss exponent. Furthermore, we, respectively, present the simulation and exact theoretical results with markers and solid lines.

TABLE I
Simulation Parameters

Symbol	Parameter name	Fixed value	Varying range
C_{th}	Sensor source rate	0.5; 1 bps/Hz	none
η	Energy harvesting efficiency	0.8	none
ρ	Power splitting factor	0.25; 0.325; 0.85; 0.925	0 to 1
λ_1	Mean of $\lvert h_{S_bR}\rvert^2$	0.1768	none
$\tilde{\lambda}_1$	Mean of $\lvert h_{RD}\rvert^2$	0.1768	none
λ_2	Mean of $\lvert h_{S_bD}\rvert^2$	1	none
$\tilde{\lambda}_2$	Mean of $\lvert h_{RE}\rvert^2$	2.7557	none
λ_3	Mean of $\lvert h_{S_bE}\rvert^2$	5.6569	none
Ψ	Transmit-power-to-noise-ratio	-5 dB	-10 to 5 (dB)
M	No. of sensor source nodes	2; 3	1 to 10
α	Path-loss exponent	2.5	none

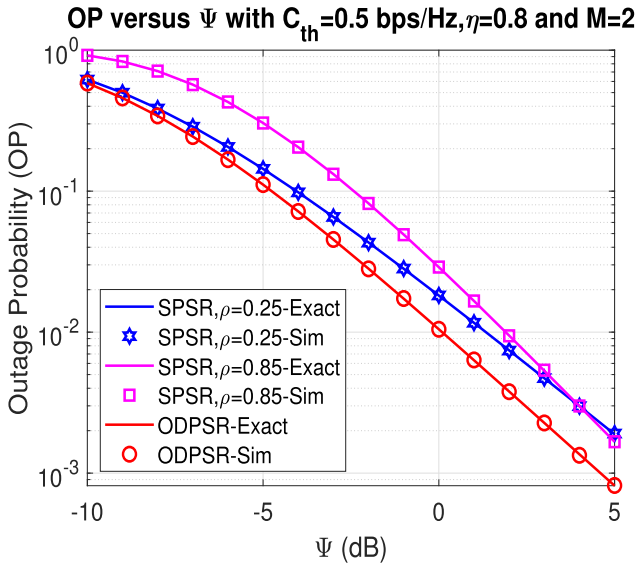

Fig. 3. OP versus Ψ with $C_{\text{th}} = 0.5$ bps/Hz, $\eta = 0.8$, and $M = 2$.

In Figs. 3 and 4, we investigate the impact of Ψ value on the OP and IP, respectively. The parameters for Figs. 3 and 4 are set as follows: $C_{\text{th}} = 0.5$ bps/Hz, $\eta = 0.8$, and $M = 2$. In Fig. 3, we compare ODPSR scheme with two SPSR schemes with fixed $\rho = 0.25$ and $\rho = 0.85$. It can be observed that the ODPSR method obtains better OP compared with others. This is expected since the proposed ODPSR can obtain the optimal ρ^* that maximizes the total capacity at the destination. It leads to a higher data rate is attained, which reduces the OP.

In Fig. 3, we can see that the system OP is dramatically decreasing when the Ψ value varies from -5 to 5 dB. This is reasonable since the higher the Ψ value is, the better the throughput can obtain. Therefore, the outage performance is enhanced. In addition, the OP of SPSR with $\rho = 0.25$ is better than that of SPSR with $\rho = 0.85$ when Ψ value is ranging

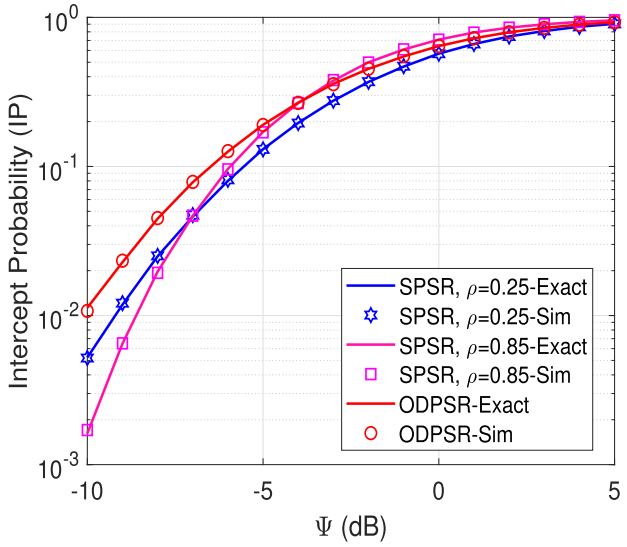

Fig. 4. IP versus Ψ with $C_{\text{th}} = 0.5$ bps/Hz, $\eta = 0.8$, and $M = 2$.

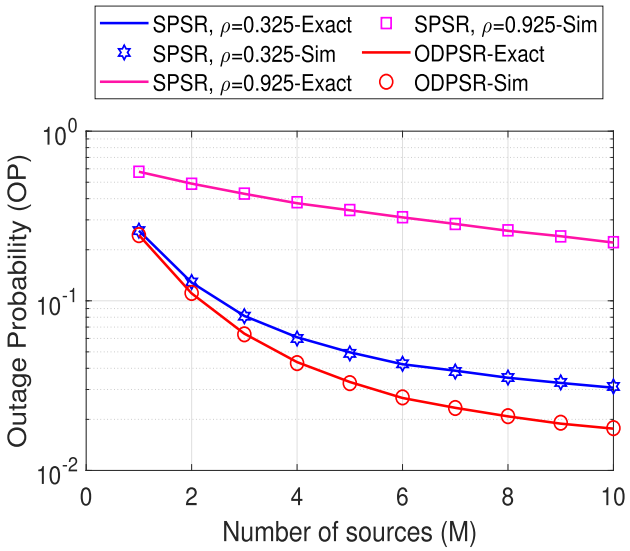

Fig. 5. OP versus number of sensor sources (M) with $C_{\text{th}} = 0.5$ bps/Hz, $\eta = 0.8$, and $\Psi = -5$ dB.

from -10 to 4 dB. However, when the transmit power is large enough, i.e., $4 \le \Psi \le 5$, SPSR with $\rho = 0.25$ is deteriorating compared to that of SPSR with $\rho = 0.85$.

In Fig. 4, the IP of ODPSR and SPSR is studied. It can be observed that intercept performance increases with a higher value of Ψ. It is expected since the eavesdropper has more chance to wiretap the channel when the sensor source S_b utilizes a higher transmit power. Moreover, when the Ψ value is large enough, all schemes can converge to a saturation value, e.g., IP $= 1$. This is due to the fact that Ψ is proportional to the IP value as in (34) and (38). One interesting thing in Fig. 4 is that the SPSR with $\rho = 0.85$ obtains the best IP performance when $\Psi < -7$ dB. When $-7 < \Psi < -4$ dB, the IP value of SPSR with $\rho = 0.25$ is lower than that of SPSR with $\rho = 0.85$, which outperforms the ODPSR method. However, the SPSR with $\rho = 0.85$ has worse performance than others when $\Psi > -4$ dB, while the SPSR with $\rho = 0.25$ is still the best one. It should be noted that the ODPSR method focuses on maximizing the capacity at the destination C_D; thus, it also minimizes the OP, as defined in (20). Nevertheless, this method is not intended to minimize the IP. Consequently, the intercept performance of the SPSR method can be better than that compared to ODPSR one, as shown in Fig. 4. In both Figs. 3 and 4, the simulation has an agreement with the analytical values, which confirms our mathematical derivations' correctness.

Figs. 5 and 6 investigate the impact of the number of sensor sources M on the OP and IP, respectively. Herein, the parameters are set as $C_{\text{th}} = 0.5$ bps/Hz, $\eta = 0.8$, and $\Psi = -5$ dB. Fig. 5 shows that the outage performance is better with a higher number of sensor sources, i.e., M varies from 1 to 10. This is because by increasing the number of sensor sources, we have more options to select the best sensor source S_b, which can enhance the transmission rate at the destination, as shown in (13). Moreover, the outage performance of ODPSR is still superior compared with other SPSR methods. As shown in Fig. 6, the number of sensor sources

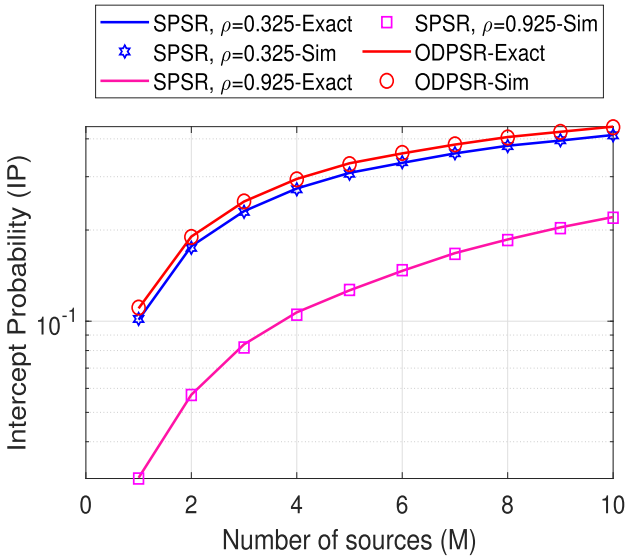

Fig. 6. IP versus number of sensor sources (M) with $C_{\text{th}} = 0.5$ bps/Hz, $\eta = 0.8$, and $\Psi = -5$ dB.

also significantly improves the IP. This shows the tradeoff between reliability and security, termed the reliability–security tradeoff (RST).

Figs. 7 and 8 illustrate the OP and IP versus the power splitting ratio ρ, with $\eta = 0.8$, $M = 3$, and $\Psi = -5$ dB. The ρ value plays an important role since it influences not only the amount of harvested energy at the relay but also the data transmission from $R \to D$. This can be explained that the higher the ρ value is, the more energy the relay can harvest. However, this also means that less power is allocated for information decoding at the relay. It leads to the fact that the OP can obtain the best value at the optimal ρ unless the performance decreases. Particularly, the OP of ODPSR obtains the best performance compared with two SPSR schemes since this method always optimizes the ρ value while designing

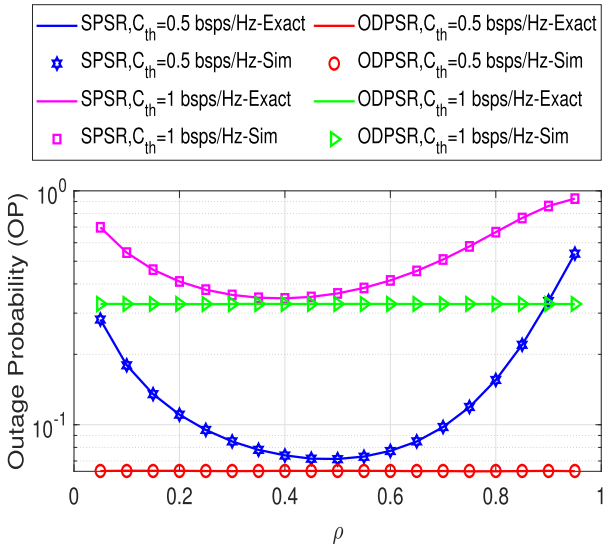

Fig. 7. OP versus power splitting ratio ρ with $\eta = 0.8$, $M = 3$, and $\Psi = -5$ dB.

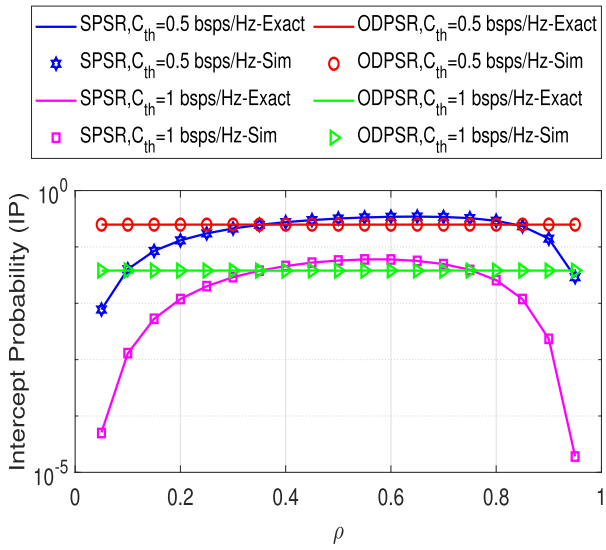

Fig. 8. IP versus power splitting ratio ρ with $\eta = 0.8$, $M = 3$, and $\Psi = -5$ dB.

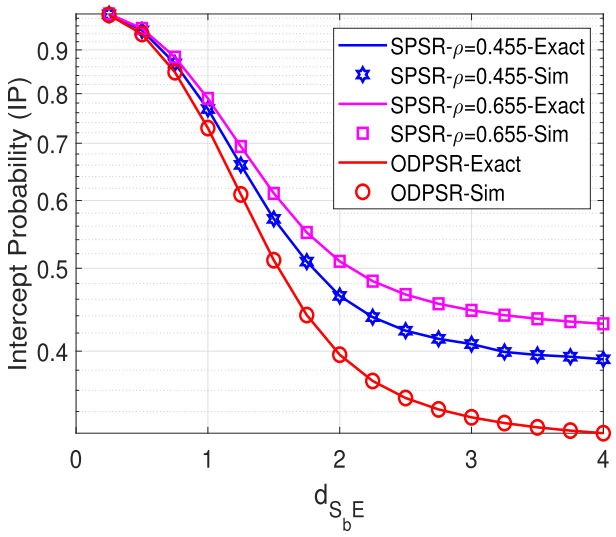

Fig. 9. IP versus distance from sensor source S_b to eavesdropper E; $d_{S_{bE}}$.

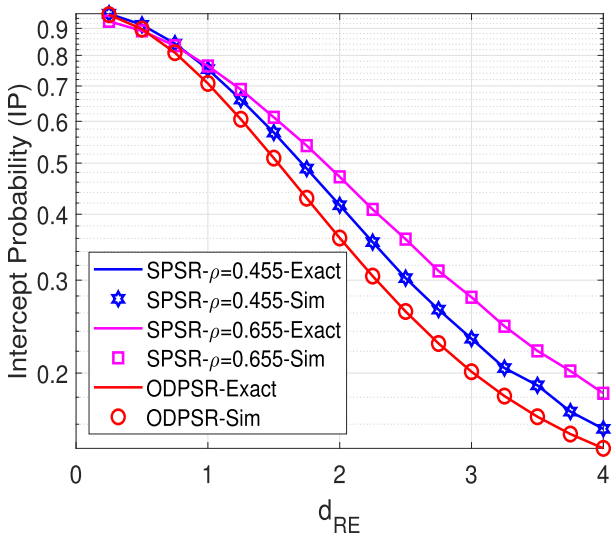

Fig. 10. IP versus distance from relay R to eavesdropper E, d_{RE}.

the system. Specifically, the optimal PS ratio $\rho^\star$ can be obtained as in Section III-B, which is calculated as the following formula $\rho^\star \triangleq (1/1 + |h_{\mathrm{RD}}|(\eta)^{1/2})$. From this equation, we see that $\rho^\star$ is a function of the channel coefficient between relay R and destination D, i.e., h_{RD}. Moreover, the OP value can be obtained by averaging over 10^6 random channel realizations. For each channel realization, we can obtain various values of $\rho^\star$, while it always fixed for SPSR. This explains the superiority of the ODPSR method over the SPSR method. The RST phenomenon also happens in Fig. 7 and 8. It is also observed from Figs. 7 and 8 that the OP and IP values of the ODPSR scheme are kept at a fixed value even we change the ρ value. This is because the ODPSR method is designed with an optimal ρ value to maximize the total throughput at the destination C_D, which describes in Section III-B. Besides, the ODPSR scheme always obtains the best OP performance, and it does not mean that it would have the worst IP performance, which is verified in Fig. 8. The ODPSR schemes have better IP value than SPSR with $C_{\mathrm{th}} = 0.5$ bps/Hz when $0.35 < \rho < 0.85$.

In Figs. 9 and 10, we investigate the influences of difference d_{S_bE} and d_{RE} to the intercept performance, respectively. Notably, since the OP expressions do not include d_{S_bE} and d_{RE}, the distance from the sensor source/relay to the eavesdropper has no effect on outage performance. It can be seen from Figs. 9 and 10 that the higher the d_{S_bE}/d_{RE} value is, the smaller the intercept performance can be obtained. It is due to the fact that the received signals at the eavesdropper are inversely proportional to the distance, as shown in (34) and (38). Moreover, the eavesdropper uses the MRC method; thus, increasing d_{S_bE} or d_{RE} still has a significant effect on intercept performance. In particular, when the distance between relay R to eavesdropper E is less than 0.5 and 0.75, the intercept performance of the ODPSR scheme is worse than

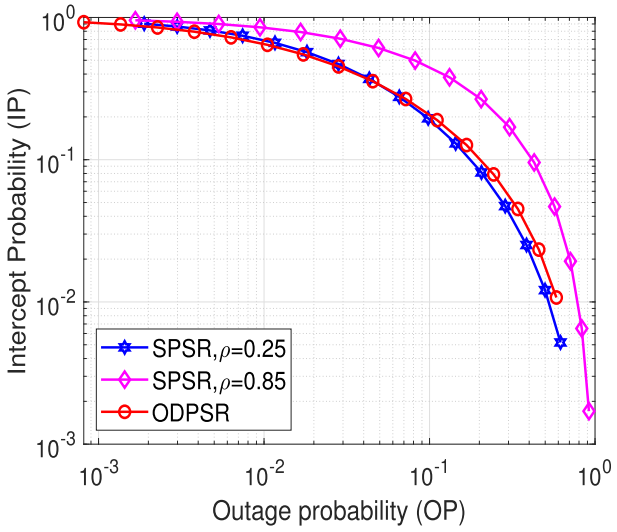

Fig. 11. IP versus OP.

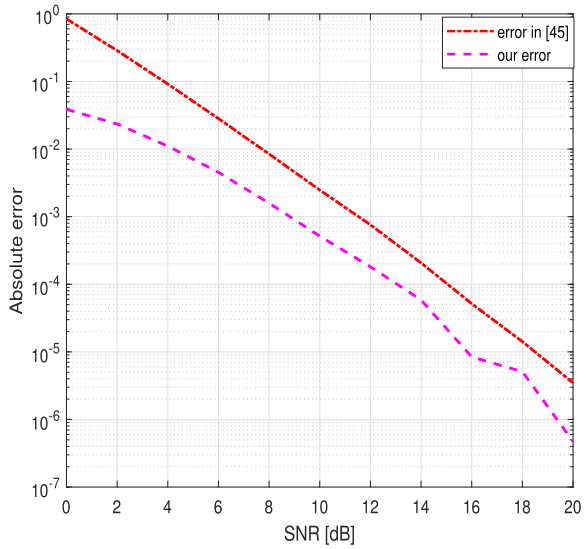

Fig. 12. Absolute error versus SNR [dB] of our proposed method and [45].

that of the SPSR with ρ equals 0.655 and 0.455, respectively. This is because the main goal of the ODPSR scheme is to maximize the capacity at the destination C_D but not to optimize the IP. Therefore, the intercept performance of the ODPSR cannot be guaranteed to be the best compared to others.

Fig. 11 illustrates the RST of ODPSR, SPSR with $\rho = 0.25$, and SPSR with $\rho = 0.85$, with $C_{\text{th}} = 0.5$ bps/Hz, $\eta = 0.8$, $\rho = 0.8$, $M = 2$, and $\Psi = -5$ dB. It can be observed from Fig. 11 that, when OP < 0.05, the IP of the SPSR with $\rho = 0.85$ is better than that of SPSR with $\rho = 0.25$. Nevertheless, when OP > 0.05, the IP of the SPSR with $\rho = 0.85$ becomes worse than SPSR with $\rho = 0.25$. Particularly, the RST of the ODPSR is always better than SPSR schemes. This shows the superiority of ODPSR over SPSR ones. Therefore, the ODPSR is preferred in practice, which provides a better RST compared to SPSR ones.

In Figs. 12 and 13, we show the gap between the simulation and analytical results of our work and [45] and [46].

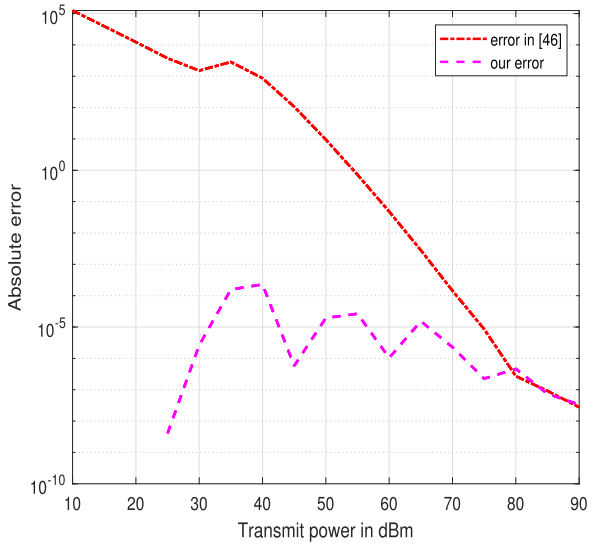

Fig. 13. Absolute error versus the transmit power of the sensor source [dBm] of our proposed method and [46].

The absolute error can be defined as the gap between simulation and analytical results, i.e., |simulation − analytical|. The simulation parameters in Fig. 12 is setting up the same as [45], where $\eta = 0.5$, $C_{\text{th}} = 0.8$, and $\Psi = 20$ dB. First, it can be observed from Fig. 12 that the absolute error of our work and [45] is significantly improved with a higher value of SNR. More specifically, when SNR equals 0 and 20 dB, the absolute error of our work (or [45]) is 0.0387 (or 0.8418) and 4.725 $e-7$ (or 3.4775 $e-6$), respectively. In particular, our work can obtain absolute error much better than that of [45] from 83.68 % to 95.4 %. Even though at low SNR (i.e., SNR equals 0 dB), our work still obtains an acceptable absolute error value, i.e., 0.0387, compared to [45], i.e., 0.8418.

In Fig. 13, we illustrate the absolute error as a function of the sensor source transmit power (in dBm). The simulation parameters in Fig. 13 are setting the same as [46], where $\eta = 0.5$, $d_{S_bD} = 35$ m, and $d_{S_bR} = d_{S_bD} - d_{\text{RD}}$. It can be observed from Fig. 13 that Ye et al. [46] obtain a very higher value of absolute error with a low transmit power of the sensor source. For instance, when the sensor source's transmit power equals 10 and 20 dBm, the absolute error of [46] imposes 1.2473 $e+5$ and 3.9303 $e+4$, which shows a large gap between simulation and mathematical formula. The absolute error of [46] is significantly decreased with a higher value of transmit power, and it can obtain a similar error as our proposed method when the transmit power is larger than 80 dBm. In contrast to [46], the absolute error in our proposed method is around 3.5123 $e-10$ to 2.2837 $e-4$, which is a very small value, and it shows the effectiveness of our method. It can be concluded from Fig. 13 that the approximation method in [46] only works well with a high transmit power of the sensor source, i.e., $P_S > 80$ dBm, while our proposed method shows the superiority in all power domains.

V. Conclusion

In this article, we have investigated the PLS for an AF-based SWIPT relay network consisting of multiple sensor sources,

an EH relay, and a destination in the presence of an eavesdropper. Specifically, we have considered the situation where both destination and eavesdropper apply the MRC method to incorporate the sensor source and relay information. By adopting the series representation of modified Bessel functions, an almost exact-form expression of the OP (for ODPSR and SPSR schemes) and IP (for SPSR) has been derived. Furthermore, we have examined the RST performance of the ODPSR and SPSR schemes in terms of the IP and OP. In general, there must be a tradeoff between the reliability (in terms of OP) and the security (in terms of IP) performance, i.e., if OP is reduced, then the IP increases. Based on the plot of OP versus IP, we can recommend suitable system parameters for satisfying the predefined requirements of IP and OP. On the other hand, the ODPSR always outperforms SPSR in terms of reliability performance because the power splitting factor ρ is selected to maximize the capacity at the destination. Although SPSR and ODPSR can be considered as two interchangeable options depending on each specific scenario, ODPSR should be preferred in general. In another aspect, an increasing number of sensor sources can provide both higher IP and OP due to more opportunities to get the best channel condition of the sensor source-relay link. If we can suppress the link from the relay to the eavesdropper, the sensor source selection will bring more benefits to the legacy link than to the wiretap link. Our work provides useful guidance regarding the RST performance to help system designers make informed decisions.

It is of interest to extend the analysis of this work to future research directions.

1) The study of a more general system model with multiple relays or multiple destinations. Even though this direction increases the computational complexity, it may further improve the system's performance.
2) Another promising direction is to consider a cluster of sensor sources with different distances to the relay.
3) The study of security enhancement by considering cooperative jammers or artificial noise by investigating SOP is an interesting problem.

Appendix A
Proof of Lemma 1

The CDF of X can be expressed as follows:

$$\begin{aligned} F_X(x) &= \Pr(X < x) \\ &= \Pr\left(\frac{\eta\rho(1-\rho)\Psi \times \max\left(\left|h_{S_bR}\right|^2\right)|h_{\mathrm{RD}}|^2}{\eta\rho|h_{\mathrm{RD}}|^2 + (1-\rho)} < x\right) \\ &= \Pr\left(\frac{\eta\rho(1-\rho)\Psi\omega_1\varphi_1}{\eta\rho\varphi_1 + (1-\rho)} < x\right) \\ &= \Pr\left(\omega_1 < \left[\frac{x(\eta\rho\varphi_1 + (1-\rho))}{\eta\rho(1-\rho)\Psi\varphi_1}\right]\right) \\ &= \int_0^\infty F_{\omega_1}\left[\frac{x(\eta\rho\varphi + (1-\rho))}{\eta\rho(1-\rho)\Psi\varphi}\right] f_{\varphi_1}(\varphi)\, d\varphi \end{aligned} \tag{41}$$

where $\varphi_1 = |h_{\mathrm{RD}}|^2$. By substituting (17) into (41), it yields

$$\begin{aligned} F_X(x) = 1 + \sum_{n=1}^{M} (-1)^n C_M^n \exp\left(-\frac{\lambda_1 n x}{(1-\rho)\Psi}\right) \\ \times \int_0^\infty \tilde{\lambda}_1 \exp\left[-\frac{\lambda_1 n x}{\eta\rho\Psi\varphi} - \tilde{\lambda}_1\varphi\right] d\varphi. \end{aligned} \tag{42}$$

By applying [61, eq. (3.324.1)], (22) is obtained, which finishes the proof.

Appendix B
Proof of Lemma 2

First, by adopting [62, eq. (1.3)], we have

$$\begin{aligned} K_\upsilon\left(2\sqrt{\frac{\lambda_1\tilde{\lambda}_1 n x}{\eta\rho\Psi}}\right) = \exp\left[-2\sqrt{\frac{\lambda_1\tilde{\lambda}_1 n x}{\eta\rho\Psi}}\right] \\ \times \sum_{l=0}^{\infty}\sum_{i=0}^{l} (2)^{2i-2\upsilon}\left[\frac{\lambda_1\tilde{\lambda}_1 n}{\eta\rho\Psi}\right]^{\frac{i-\upsilon}{2}} \\ \times \Lambda(\upsilon, l, i)\, x^{\frac{i-\upsilon}{2}} \end{aligned} \tag{43}$$

where $\Lambda(\upsilon,l,i) = ((-1)^i(\pi)^{1/2}\Gamma(2\upsilon)\Gamma(l-\upsilon+1/2)L(l,i))/(\Gamma(1/2-\upsilon)\Gamma(1/2+l+\upsilon)i!)$, and $L(l,j) = \binom{l-1}{j-1}(l!/j!)$ is the coefficient, namely, the Lah number [62]. Then, the function $\exp(-2((\lambda_1\tilde{\lambda}_1 n x/\eta\rho\Psi))^{1/2})$ is transformed by applying the Taylor series [61, eq. (1.211.1)] as follows:

$$\begin{aligned} \exp\left(-2\sqrt{\frac{\lambda_1\tilde{\lambda}_1 n x}{\eta\rho\Psi}}\right) &= \sum_{t=0}^{\infty} \frac{\left(-2\sqrt{\frac{\lambda_1\tilde{\lambda}_1 n x}{\eta\rho\Psi}}\right)^t}{t!} \\ &= \sum_{t=0}^{\infty}\left[\frac{\lambda_1\tilde{\lambda}_1 n}{\eta\rho\Psi}\right]^{t/2} \frac{(-1)^t(2)^t x^{t/2}}{t!}. \end{aligned} \tag{44}$$

By applying (30), the integral in (25) can be reformulated by

$$\begin{aligned} \Xi = \sum_{t=0}^{\infty}\sum_{l=0}^{\infty}\sum_{i=0}^{l} \frac{(-1)^t(2)^{2i-2+t}\Lambda(1,l,i)}{t!}\left[\frac{\lambda_1\tilde{\lambda}_1 n}{\eta\rho\Psi}\right]^{\frac{i+t}{2}} \\ \times \int_0^{\gamma_{th}} x^{\frac{i+t}{2}} \exp\left(\frac{\lambda_2 x}{\Psi} - \frac{\lambda_1 n x}{(1-\rho)\Psi}\right) dx. \end{aligned} \tag{45}$$

By applying [61, eq. (3.324.1)], Ξ can be described by

$$\begin{aligned} \Xi = \sum_{t=0}^{\infty}\sum_{l=0}^{\infty}\sum_{i=0}^{l} \frac{(-1)^t(2)^{2i-2+t}\Lambda(1,l,i)}{t!} \times \left[\frac{\lambda_1\tilde{\lambda}_1 n}{\eta\rho\Psi}\right]^{\frac{i+t}{2}} \\ \times \left[\frac{\lambda_1 n}{(1-\rho)\Psi} - \frac{\lambda_2}{\Psi}\right]^{\left(-\frac{i+t+2}{2}\right)} \\ \times \gamma\left(\frac{i+t+2}{2}, \left[\frac{\lambda_1 n}{(1-\rho)\Psi} - \frac{\lambda_2}{\Psi}\right]\gamma_{th}\right) \end{aligned} \tag{46}$$

where $\gamma(s,x) = \int_0^x t^{s-1}e^{-t}dt$ is the lower incomplete gamma function. Next, by substituting (46) into (25), the OP can be, finally, obtained by (26).

APPENDIX C
PROOF OF LEMMA 3

The CDF of $\widetilde{X}$ can be expressed as

$$\begin{aligned} F_{\widetilde{X}}(\widetilde{x}) &= \Pr\left[\frac{\eta\Psi\omega_1\varphi_1}{\left(1+\sqrt{\eta\varphi_1}\right)^2} < \widetilde{x}\right] \\ &= \Pr\left[\omega_1 < \frac{\widetilde{x}\left(1+\sqrt{\eta\varphi_1}\right)^2}{\eta\Psi\varphi_1}\right] \\ &= \int_0^{\infty} F_{\omega_1}\left[\frac{\widetilde{x}\left(1+\sqrt{\eta\widetilde{y}}\right)^2}{\eta\Psi\widetilde{y}}\right] \times f_{\varphi_1}(\widetilde{y})\, d\widetilde{y}. \quad (47) \end{aligned}$$

By applying (17), (47) can be rewritten as

$$\begin{aligned} F_{\widetilde{X}}(\widetilde{x}) = 1 + \sum_{n=1}^{M} (-1)^n C_M^n \tilde{\lambda}_1 \times \exp\left(-\frac{\lambda_1 n\widetilde{x}}{\Psi}\right) \\ \times \int_0^{\infty} \exp\left(-\frac{\lambda_1 n\widetilde{x}}{\eta\Psi\widetilde{y}}\right) \exp\left(-\frac{2\lambda_1 n\widetilde{x}}{\Psi\sqrt{\eta\widetilde{y}}}\right) \\ \times \exp\left(-\tilde{\lambda}_1\widetilde{y}\right) d\widetilde{y}. \quad (48) \end{aligned}$$

Then, the Taylor series is adopted to make (48) tractability as follows:

$$\begin{aligned} \exp\left(-\frac{2\lambda_1 n\widetilde{x}}{\Psi\sqrt{\eta\widetilde{y}}}\right) &= \sum_{k=0}^{\infty} \frac{\left(-\frac{2\lambda_1 n\widetilde{x}}{\Psi\sqrt{\eta\widetilde{y}}}\right)^k}{k!} \\ &= \sum_{k=0}^{\infty} \frac{(-1)^k (2\lambda_1 n\widetilde{x})^k}{\Psi^k \eta^{k/2} k!} \widetilde{y}^{-k/2}. \quad (49) \end{aligned}$$

By substituting (49) into (48), we have

$$\begin{aligned} F_{\widetilde{X}}(\widetilde{x}) \\ = 1 + \sum_{k=0}^{\infty}\sum_{n=1}^{M} \frac{(-1)^{k+n} C_M^n (2\lambda_1 n\widetilde{x})^k \tilde{\lambda}_1}{\Psi^k \eta^{k/2} k!} \exp\left(-\frac{\lambda_1 n\widetilde{x}}{\Psi}\right) \\ \times \int_0^{\infty} \widetilde{y}^{-k/2} \exp\left(-\frac{\lambda_1 n\widetilde{x}}{\eta\Psi\widetilde{y}}\right) \exp\left(-\tilde{\lambda}_1\widetilde{y}\right) d\widetilde{y}. \quad (50) \end{aligned}$$

The CDF of $\widetilde{X}$ is, finally, obtained as in (29) by applying [61, eq. (3.471.9)].

APPENDIX D
PROOF OF THEOREM 1

Similar to (43), we have

$$\begin{aligned} K_q\left(2\sqrt{\frac{\lambda_1\tilde{\lambda}_1 n\widetilde{x}}{\eta\Psi}}\right) = \exp\left[-2\sqrt{\frac{\lambda_1\tilde{\lambda}_1 n\widetilde{x}}{\eta\Psi}}\right] \\ \times \sum_{l=0}^{\infty}\sum_{i=0}^{l} (2)^{2i-2q} \left[\frac{\lambda_1\tilde{\lambda}_1 n}{\eta\Psi}\right]^{\frac{i-q}{2}} \\ \times \Lambda(q,l,i)\, \widetilde{x}^{\frac{i-q}{2}} \quad (51) \end{aligned}$$

where $q = -k/2 + 1$.

Next, by adopting [61, eq. (1.211.1)], we obtain

$$\begin{aligned} \exp\left(-2\sqrt{\frac{\lambda_1\tilde{\lambda}_1 n\widetilde{x}}{\eta\Psi}}\right) &= \sum_{t=0}^{\infty} \frac{\left(-2\sqrt{\frac{\lambda_1\tilde{\lambda}_1 n\widetilde{x}}{\eta\Psi}}\right)^t}{t!} \\ &= \sum_{t=0}^{\infty} \left[\frac{\lambda_1\tilde{\lambda}_1 n}{\eta\Psi}\right]^{t/2} \frac{(-1)^t (2)^t \widetilde{x}^{t/2}}{t!}. \end{aligned} \quad (52)$$

By substituting (52) into (51), we have

$$\begin{aligned} K_q\left(2\sqrt{\frac{\lambda_1\tilde{\lambda}_1 n\widetilde{x}}{\eta\Psi}}\right) \\ = \sum_{t=0}^{\infty}\sum_{l=0}^{\infty}\sum_{i=0}^{l} \left\{ \begin{array}{l} \frac{(-1)^t (2)^{2i-2q+t}}{t!} \times \left[\frac{\lambda_1\tilde{\lambda}_1 n}{\eta\Psi}\right]^{\frac{i-q+t}{2}} \\ \times \Lambda(q,l,i)\, \widetilde{x}^{\frac{i-q+t}{2}} \end{array} \right. \quad (53) \end{aligned}$$

Then, by substituting (53) into (31), $\mathrm{OP}^{\mathrm{ODPSR}}$ can be expressed as

$$\begin{aligned} \mathrm{OP}^{\mathrm{ODPSR}} \\ = 1 - \exp\left(-\frac{\lambda_2\gamma_{th}}{\Psi}\right) + \widetilde{\sum}^{*} \frac{(-1)^{k+n+t} 2^{2i+2k+t-1} C_M^n \lambda_2}{k!t!\Psi} \\ \times \left(\frac{\tilde{\lambda}_1}{\eta}\right)^{\frac{k+i+t}{2}} \left(\frac{\lambda_1 n}{\Psi}\right)^{\frac{2k+i+t}{2}} \exp\left(-\frac{\lambda_2\gamma_{th}}{\Psi}\right) \\ \times \Lambda(q,l,i) \int_0^{\gamma_{th}} \widetilde{x}^{\frac{i+t+2k}{2}} \exp\left[-\widetilde{x}\left(\frac{\lambda_1 nx}{\Psi} - \frac{\lambda_2\widetilde{x}}{\Psi}\right)\right] d\widetilde{x} \end{aligned} \quad (54)$$

where $\widetilde{\sum}^{*} = \sum_{k=0}^{\infty}\sum_{t=0}^{\infty}\sum_{l=0}^{\infty}\sum_{i=0}^{l}\sum_{n=1}^{M}$. Finally, by applying [61, eq. (3.324.1)], $\mathrm{OP}^{\mathrm{ODPSR}}$ is expressed as in (32), which finishes the proof.

APPENDIX E
PROOF OF LEMMA 4

First, the CDF of T is expressed as follows:

$$\begin{aligned} F_T(t) = \Pr(T < t) = \Pr\left(\frac{\frac{\eta\tilde{\varphi}_1}{1+\tilde{\varphi}_1}\Psi\omega_1\varphi_2}{\eta\varphi_2 + \tilde{\varphi}_1} < t\right) \\ = \int_0^{\infty} \underbrace{\Pr\left(\frac{\frac{\eta x}{1+x}\Psi\omega_1\varphi_2}{\eta\varphi_2 + x} < t\right)}_{P(x)} f_{\tilde{\varphi}_1}(x)\, dx. \quad (55) \end{aligned}$$

The probability $P(x)$ in (55) can be calculated as

$$\begin{aligned} P(x) = \Pr\left(\frac{\frac{\eta x}{1+x}\Psi\omega_1\varphi_2}{\eta\varphi_2 + x} < t\right) \\ = \int_0^{\infty} F_{\omega_1}\left(\frac{t(\eta\varphi + x)(1+x)}{\eta x\Psi\varphi} | \varphi_2 = \varphi\right) f_{\varphi_2}(\varphi) d\varphi. \end{aligned} \quad (56)$$

Then, by adopting (17), $P(x)$ can be reformulated as

$$\begin{aligned} P(x) &= 1+\sum_{n=1}^{M}(-1)^n C_M^n \tilde{\lambda}_2 \int_0^{\infty} \left\{ \begin{array}{l} \exp\left[-\frac{\lambda_1 nt(\eta\varphi+x)(1+x)}{\eta x \Psi \varphi}\right] \\ \times \exp\left(-\tilde{\lambda}_2\varphi\right) d\varphi \end{array} \right\} \\ &= 1+\sum_{n=1}^{M}(-1)^n C_M^n \tilde{\lambda}_2 \exp\left(-\frac{\lambda_1 nt\,(1+x)}{x\Psi}\right) \\ &\quad \times \int_0^{\infty} \exp\left(-\frac{\lambda_1 nt\,(1+x)}{\eta\Psi\varphi} - \tilde{\lambda}_2\varphi\right) d\varphi. \end{aligned} \tag{57}$$

Equation (57) can be obtained by applying [61, eq. (3.324.1)] as follows:

$$\begin{aligned} P(x) = 1+2\sum_{n=1}^{M}(-1)^n C_M^n \exp\left(-\frac{\lambda_1 nt\,(1+x)}{x\Psi}\right) \\ \times \sqrt{\frac{\lambda_1\tilde{\lambda}_2 nt\,(1+x)}{\eta\Psi}} \times K_1\left(2\sqrt{\frac{\lambda_1\tilde{\lambda}_2 nt\,(1+x)}{\eta\Psi}}\right). \end{aligned} \tag{58}$$

Next, the CDF of $\tilde{\varphi}_1$ can be derived as

$$\begin{aligned} F_{\tilde{\varphi}_1}(x) &= \Pr(\tilde{\varphi}_1 < x) = \Pr\left(\sqrt{\eta\varphi_1} < x\right) \\ &= \Pr\left(\varphi_1 < \frac{x^2}{\eta}\right) = 1-\exp\left(-\frac{\tilde{\lambda}_1 x^2}{\eta}\right). \end{aligned} \tag{59}$$

Then, the corresponding pdf of $\tilde{\varphi}_1$ can be calculated by

$$f_{\tilde{\varphi}_1}(x) = \frac{\partial F_{\tilde{\varphi}_1}(x)}{\partial x} = \frac{2\tilde{\lambda}_1 x}{\eta}\exp\left(-\frac{\tilde{\lambda}_1 x^2}{\eta}\right). \tag{60}$$

By substituting (58) and (60) into (55), $F_T(t)$ can be rewritten as

$$\begin{aligned} F_T(t) = 1+4\sum_{n=1}^{M}(-1)^n C_M^n \exp\left(-\frac{\lambda_1 nt}{\Psi}\right) \\ \times \int_0^{\infty} \frac{\tilde{\lambda}_1 x}{\eta}\exp\left(-\frac{\lambda_1 nt}{x\Psi}\right)\exp\left(-\frac{\tilde{\lambda}_1 x^2}{\eta}\right) \\ \times \sqrt{\frac{\lambda_1\tilde{\lambda}_2 nt\,(1+x)}{\eta\Psi}} K_1\left(2\sqrt{\frac{\lambda_1\tilde{\lambda}_2 nt\,(1+x)}{\eta\Psi}}\right) dx. \end{aligned} \tag{61}$$

From (61), the Taylor series is applied for exponential function as follows:

$$\exp\left(-\frac{\lambda_1 nt}{x\Psi}\right) = \sum_{s=0}^{\infty}\frac{\left(-\frac{\lambda_1 nt}{x\Psi}\right)^s}{s!} = \sum_{s=0}^{\infty}\frac{(-1)^s\left(\frac{\lambda_1 nt}{\Psi}\right)^s}{s!}x^{-s} \tag{62}$$

$$\exp\left(-\frac{\tilde{\lambda}_1 x^2}{\eta}\right) = \sum_{r=0}^{\infty}\frac{\left(-\frac{\tilde{\lambda}_1 x^2}{\eta}\right)^r}{r!} = \sum_{s=0}^{\infty}\frac{(-1)^r\left(\frac{\tilde{\lambda}_1}{\eta}\right)^r}{r!}x^{2r}. \tag{63}$$

By replacing (62) and (63) into (61), it yields

$$\begin{aligned} F_T(t) = 1+4\sum_{r=0}^{\infty}\sum_{s=0}^{\infty}\sum_{n=1}^{M}\frac{(-1)^{n+s+r}C_M^n \exp\left(-\frac{\lambda_1 nt}{\Psi}\right)}{r!s!} \\ \times\left(\frac{\lambda_1 nt}{\Psi}\right)^{s+1/2}\left(\frac{\tilde{\lambda}_1}{\eta}\right)^{r+1}\sqrt{\frac{\tilde{\lambda}_2}{\eta}} \\ \times\int_0^{\infty} x^{2r-s+1}(x+1)^{1/2}K_1\left(2\sqrt{\frac{\lambda_1\tilde{\lambda}_2 nt\,(x+1)}{\eta\Psi}}\right) dx. \end{aligned} \tag{64}$$

Finally, (37) can be obtained by using [61, eq. (6.592.4)], and (64) finishes the proof.

ACKNOWLEDGMENT

Tan N. Nguyen is with the Communication and Signal Processing Research Group, Faculty of Electrical and Electronics Engineering, Ton Duc Thang University, Ho Chi Minh City 72900, Vietnam (e-mail: nguyennhattan@tdtu.edu.vn).

Dinh-Hieu Tran was with the Interdisciplinary Centre for Security, Reliability and Trust (SnT), University of Luxembourg, 4365 Esch-sur-Alzette, Luxembourg. He is now with Nokia Bell Labs, 91300 Massy, France (e-mail: dinh-hieu.tran@nokia.com).

Trinh Van Chien is with the School of Information and Communication Technology (SoICT), Hanoi University of Science and Technology, Hanoi 100000, Vietnam (e-mail: chientv@soict.hust.edu.vn).

Van-Duc Phan is with the Faculty of Automotive Engineering, School of Engineering and Technology, Van Lang University, Ho Chi Minh City 700000, Vietnam (email: duc.pv@vlu.edu.vn).

Nhat-Tien Nguyen and Miroslav Voznak are with the Faculty of Electrical Engineering and Computer Science, VSB—Technical University of Ostrava, 70800 Ostrava, Czech Republic (e-mail: nguyen.nhat.tien.st@vsb.cz; miroslav.voznak@vsb.cz).

Symeon Chatzinotas and Björn Ottersten are with the Interdisciplinary Centre for Security, Reliability and Trust (SnT), University of Luxembourg, 4365 Esch-sur-Alzette, Luxembourg (e-mail: symeon.chatzinotas@uni.lu; bjorn.ottersten@uni.lu).

H. Vincent Poor is with the Electrical Engineering Department, Princeton University, Princeton, NJ 08544 USA (e-mail: poor@princeton.edu).

REFERENCES

[1] *Ericsson Mobility Report: November 2019*, Ericsson, Stockholm, Sweden, 2019.

[2] D.-H. Tran, V.-D. Nguyen, S. Gautam, S. Chatzinotas, T. X. Vu, and B. Ottersten, "UAV relay-assisted emergency communications in IoT networks: Resource allocation and trajectory optimization," 2020, *arXiv:2008.00218*.

[3] T. H. Nguyen, W.-S. Jung, L. T. Tu, T. Van Chien, D. Yoo, and S. Ro, "Performance analysis and optimization of the coverage probability in dual hop LoRa networks with different fading channels," *IEEE Access*, vol. 8, pp. 107087–107102, 2020.

[4] T. D. Hieu and B.-S. Kim, "Stability-aware geographic routing in energy harvesting wireless sensor networks," *Sensors*, vol. 16, no. 5, p. 696, 2016.

[5] S. Bi, C. K. Ho, and R. Zhang, "Wireless powered communication: Opportunities and challenges," *IEEE Commun. Mag.*, vol. 53, no. 4, pp. 117–125, Apr. 2015.

[6] D. Niyato, D. I. Kim, M. Maso, and Z. Han, "Wireless powered communication networks: Research directions and technological approaches," *IEEE Wireless Commun.*, vol. 24, no. 6, pp. 88–97, Dec. 2017.

[7] P. X. Nguyen et al., "Backscatter-assisted data offloading in OFDMA-based wireless-powered mobile edge computing for IoT networks," *IEEE Internet Things J.*, vol. 8, no. 11, pp. 9233–9243, Jun. 2021.

[8] L. R. Varshney, "Transporting information and energy simultaneously," in *Proc. IEEE Int. Symp. Inf. Theory*, Jul. 2008, pp. 1612–1616.

[9] P. Grover and A. Sahai, "Shannon meets tesla: Wireless information and power transfer," in *Proc. IEEE Int. Symp. Inf. Theory*, Jun. 2010, pp. 2363–2367.

[10] R. Zhang and C. K. Ho, "MIMO broadcasting for simultaneous wireless information and power transfer," *IEEE Trans. Wireless Commun.*, vol. 12, no. 5, pp. 1989–2001, Mar. 2013.

[11] L. Dai, B. Wang, M. Peng, and S. Chen, "Hybrid precoding-based millimeter-wave massive MIMO-NOMA with simultaneous wireless information and power transfer," *IEEE J. Sel. Areas Commun.*, vol. 37, no. 1, pp. 131–141, Jan. 2019.

[12] C. Pan et al., "Intelligent reflecting surface aided MIMO broadcasting for simultaneous wireless information and power transfer," *IEEE J. Sel. Areas Commun.*, vol. 38, no. 8, pp. 1719–1734, Aug. 2020.

[13] P. Raut, P. K. Sharma, T. A. Tsiftsis, and Y. Zou, "Power-time splitting-based non-linear energy harvesting in FD short-packet communications," *IEEE Trans. Veh. Technol.*, vol. 69, no. 8, pp. 9146–9151, Aug. 2020.

[14] E. Boshkovska, D. W. K. Ng, N. Zlatanov, A. Koelpin, and R. Schober, "Robust resource allocation for MIMO wireless powered communication networks based on a non-linear EH model," *IEEE Trans. Commun.*, vol. 65, no. 5, pp. 1984–1999, May 2017.

[15] X. Zhang, Y. Wang, F. Zhou, N. Al-Dhahir, and X. Deng, "Robust resource allocation for MISO cognitive radio networks under two practical non-linear energy harvesting models," *IEEE Commun. Lett.*, vol. 22, no. 9, pp. 1874–1877, Sep. 2018.

[16] F. Zhou, Z. Chu, H. Sun, R. Q. Hu, and L. Hanzo, "Artificial noise aided secure cognitive beamforming for cooperative MISO-NOMA using SWIPT," *IEEE Trans. J. Sel. Areas. Commum.*, vol. 36, no. 4, pp. 918–931, Apr. 2018.

[17] X. Zhou, R. Zhang, and C. K. Ho, "Wireless information and power transfer: Architecture design and rate-energy tradeoff," *IEEE Trans. Commun.*, vol. 61, no. 11, pp. 4754–4767, Nov. 2013.

[18] L. Shi, W. Cheng, Y. Ye, H. Zhang, and R. Q. Hu, "Heterogeneous power-splitting based two-way DF relaying with non-linear energy harvesting," in *Proc. IEEE Global Commun. Conf. (GLOBECOM)*, Dec. 2018, pp. 1–7.

[19] S. Solanki, P. K. Upadhyay, D. B. D. Costa, H. Ding, and J. M. Moualeu, "Performance analysis of piece-wise linear model of energy harvesting-based multiuser overlay spectrum sharing networks," *IEEE Open J. Commun. Soc.*, vol. 1, pp. 1820–1836, 2020.

[20] A. K. Shukla, V. Singh, P. K. Upadhyay, A. Kumar, and J. M. Moualeu, "Performance analysis of energy harvesting-assisted overlay cognitive NOMA systems with incremental relaying," *IEEE Open J. Commun. Soc.*, vol. 2, pp. 1558–1576, 2021.

[21] Y. Huang, J. Wang, C. Zhong, T. Q. Duong, and G. K. Karagiannidis, "Secure transmission in cooperative relaying networks with multiple antennas," *IEEE Trans. Wireless Commun.*, vol. 15, no. 10, pp. 6843–6856, Oct. 2016.

[22] L. Dong, Z. Han, A. P. Petropulu, and H. V. Poor, "Improving wireless physical layer security via cooperating relays," *IEEE Trans. Signal Process.*, vol. 58, no. 3, pp. 1875–1888, Mar. 2010.

[23] T. M. Hoang et al., "Security and energy harvesting for MIMO-OFDM networks," *IEEE Trans. Commun.*, vol. 68, no. 4, pp. 2593–2606, Apr. 2020.

[24] X. Li, M. Zhao, Y. Liu, L. Li, Z. Ding, and A. Nallanathan, "Secrecy analysis of ambient backscatter NOMA systems under I/Q imbalance," *IEEE Trans. Veh. Technol.*, vol. 69, no. 10, pp. 12286–12290, Oct. 2020.

[25] K. J. Kim, H. Liu, M. Wen, P. V. Orlik, and H. V. Poor, "Secrecy performance analysis of distributed asynchronous cyclic delay diversity-based cooperative single carrier systems," *IEEE Trans. Commun.*, vol. 68, no. 5, pp. 2680–2694, May 2020.

[26] H.-M. Wang and X.-G. Xia, "Enhancing wireless secrecy via cooperation: Signal design and optimization," *IEEE Commun. Mag.*, vol. 53, no. 12, pp. 47–53, Dec. 2015.

[27] D.-H. Ha, T. N. Nguyen, M. H. Q. Tran, X. Li, P. T. Tran, and M. Voznak, "Security and reliability analysis of a two-way half-duplex wireless relaying network using partial relay selection and hybrid TPSR energy harvesting at relay nodes," *IEEE Access*, vol. 8, pp. 187165–187181, 2020.

[28] D. R. Pattanayak, V. K. Dwivedi, V. Karwal, I. S. Ansari, H. Lei, and M.-S. Alouini, "On the physical layer security of a decode and forward based mixed FSO/RF co-operative system," *IEEE Wireless Commun. Lett.*, vol. 9, no. 7, pp. 1031–1035, Jul. 2020.

[29] M. H. Khoshafa, T. M. N. Ngatched, and M. H. Ahmed, "On the physical layer security of underlay relay-aided device-to-device communications," *IEEE Trans. Veh. Technol.*, vol. 69, no. 7, pp. 7609–7621, Jul. 2020.

[30] T. N. Nguyen et al., "Performance enhancement for energy harvesting based two-way relay protocols in wireless ad-hoc networks with partial and full relay selection methods," *Ad Hoc Netw.*, vol. 84, pp. 178–187, Mar. 2019.

[31] H. Dinh Tran, D. Trung Tran, and S. G. Choi, "Secrecy performance of a generalized partial relay selection protocol in underlay cognitive networks," *Int. J. Commun. Syst.*, vol. 31, no. 17, Nov. 2018, Art. no. e3806.

[32] T. N. Nguyen, M. Tran, T. Nguyen, and M. Voznak, "Adaptive relaying protocol for decode and forward full-duplex system over Rician fading channel: System performance analysis," *China Commun.*, vol. 16, no. 3, pp. 92–102, 2019.

[33] T. N. Nguyen, P. T. Tran, and M. Voznak, "Wireless energy harvesting meets receiver diversity: A successful approach for two-way half-duplex relay networks over block Rayleigh fading channel," *Comput. Netw.*, vol. 172, May 2020, Art. no. 107176.

[34] K. Cao, B. Wang, H. Ding, T. Li, and F. Gong, "Optimal relay selection for secure NOMA systems under untrusted users," *IEEE Trans. Veh. Technol.*, vol. 69, no. 2, pp. 1942–1955, Feb. 2020.

[35] A. Arafa, W. Shin, M. Vaezi, and H. V. Poor, "Secure relaying in non-orthogonal multiple access: Trusted and untrusted scenarios," *IEEE Trans. Inf. Forensics Security*, vol. 15, pp. 210–222, 2020.

[36] A. Arafa, E. Panayirci, and H. V. Poor, "Relay-aided secure broadcasting for visible light communications," *IEEE Trans. Commun.*, vol. 67, no. 6, pp. 4227–4239, Jun. 2019.

[37] T. X. Zheng, H. M. Wang, F. Liu, and M. H. Lee, "Outage constrained secrecy throughput maximization for DF relay networks," *IEEE Trans. Commun.*, vol. 63, no. 5, pp. 1741–1755, May 2015.

[38] H.-M. Wang, K.-W. Huang, Q. Yang, and Z. Han, "Joint source-relay secure precoding for MIMO relay networks with direct links," *IEEE Trans. Commun.*, vol. 65, no. 7, pp. 2781–2793, Jul. 2017.

[39] T. D. Hieu, T. T. Duy, and B.-S. Kim, "Performance enhancement for multihop harvest-to-transmit WSNs with path-selection methods in presence of eavesdroppers and hardware noises," *IEEE Sensors J.*, vol. 18, no. 12, pp. 5173–5186, Jun. 2018.

[40] V. N. Vo, T. G. Nguyen, C. So-In, and D.-B. Ha, "Secrecy performance analysis of energy harvesting wireless sensor networks with a friendly jammer," *IEEE Access*, vol. 5, pp. 25196–25206, 2017.

[41] Z. Mobini, M. Mohammadi, and C. Tellambura, "Wireless-powered full-duplex relay and friendly jamming for secure cooperative communications," *IEEE Trans. Inf. Forensics Security*, vol. 14, no. 3, pp. 621–634, Mar. 2019.

[42] K. Cao et al., "Improving physical layer security of uplink NOMA via energy harvesting jammers," *IEEE Trans. Inf. Forensics Security*, vol. 16, pp. 786–799, 2021.

[43] A. A. Okandeji, M. R. A. Khandaker, K.-K. Wong, G. Zheng, Y. Zhang, and Z. Zheng, "Secure full-duplex two-way relaying for SWIPT," *IEEE Wireless Commun. Lett.*, vol. 7, no. 3, pp. 336–339, Jun. 2018.

[44] K. Lee, J.-P. Hong, H.-H. Choi, and T. Q. S. Quek, "Wireless-powered two-way relaying protocols for optimizing physical layer security," *IEEE Trans. Inf. Forensics Security*, vol. 14, no. 1, pp. 162–174, Jan. 2019.

[45] H. Lee, C. Song, S.-H. Choi, and I. Lee, "Outage probability analysis and power splitter designs for SWIPT relaying systems with direct link," *IEEE Commun. Lett.*, vol. 21, no. 3, pp. 648–651, Mar. 2017.

[46] Y. Ye, Y. Li, F. Zhou, N. Al-Dhahir, and H. Zhang, "Power splitting-based SWIPT with dual-hop DF relaying in the presence of a direct link," *IEEE Syst. J.*, vol. 13, no. 2, pp. 1316–1319, Jun. 2019.

[47] P. Yan, Y. Zou, X. Ding, and J. Zhu, "Energy-aware relay selection improves security-reliability tradeoff in energy harvesting cooperative cognitive radio systems," *IEEE Trans. Veh. Technol.*, vol. 69, no. 5, pp. 5115–5128, May 2020.

[48] Z. Cao et al., "Security-reliability trade-off analysis of AN-aided relay selection for full-duplex relay networks," *IEEE Trans. Veh. Technol.*, vol. 70, no. 3, pp. 2362–2377, Mar. 2021.

[49] B. Li, Y. Zou, J. Zhu, and W. Cao, "Impact of hardware impairment and co-channel interference on security-reliability trade-off for wireless sensor networks," *IEEE Trans. Wireless Commun.*, vol. 20, no. 11, pp. 7011–7025, Nov. 2021.

[50] T. N. Nguyen, T. H. Q. Minh, P. T. Tran, and M. Voznak, "Adaptive energy harvesting relaying protocol for two-way half-duplex system network over Rician fading channels," *Wireless Commun. Mobile Comput.*, vol. 2018, pp. 1–10, Apr. 2018.

[51] T. Nguyen et al., "Hybrid TSR–PSR alternate energy harvesting relay network over rician fading channels: Outage probability and SER analysis," *Sensors*, vol. 18, no. 11, p. 3839, Nov. 2018.

[52] P. T. Tin, B. H. Dinh, T. N. Nguyen, D. H. Ha, and T. T. Trang, "Power beacon-assisted energy harvesting wireless physical layer cooperative relaying networks: Performance analysis," *Symmetry*, vol. 12, no. 1, p. 106, Jan. 2020.

[53] C. Trinh et al., "Joint pilot design and uplink power allocation in multi-cell massive MIMO systems," *IEEE Trans. Wireless Commun.*, vol. 17, no. 3, pp. 2000–2015, Jan. 2018.

[54] Z. Yang and X. Wang, "A sequential Monte Carlo blind receiver for OFDM systems in frequency-selective fading channels," *IEEE Trans. Signal Process.*, vol. 50, no. 2, pp. 271–280, Feb. 2002.

[55] B. Renfei, W. Shilian, and Y. Xiaoyou, "Blind channel estimation and phase ambiguity elimination in MIMO-OFDM UWA communications," in *Proc. IEEE Int. Conf. Signal Process., Commun. Comput. (ICSPCC)*, Aug. 2016, pp. 1–6.

[56] A. Salem, K. A. Hamdi, and K. M. Rabie, "Physical layer security with RF energy harvesting in AF multi-antenna relaying networks," *IEEE Trans. Commun.*, vol. 64, no. 7, pp. 3025–3038, Jul. 2016.
[57] N. Zhao, F. Hu, Z. Li, and Y. Gao, "Simultaneous wireless information and power transfer strategies in relaying network with direct link to maximize throughput," *IEEE Trans. Veh. Technol.*, vol. 67, no. 9, pp. 8514–8524, Sep. 2018.
[58] H. Tran-Dinh, S. Gautam, S. Chatzinotas, and B. Ottersten, "Throughput maximization for wireless communication systems with backscatter- and cache-assisted UAV technology," 2020, *arXiv:2011.07955*.
[59] T. N. Nguyen et al., "Security–reliability tradeoff analysis for SWIPT- and AF-based IoT networks with friendly jammers," *IEEE Internet Things J.*, vol. 9, no. 21, pp. 21662–21675, Nov. 2022.
[60] Z. Fang, Y. Wu, Y. Lu, J. Hu, T. Peng, and J. Ye, "Simultaneous wireless information and power transfer in cellular two-way relay networks with massive MIMO," *IEEE Access*, vol. 6, pp. 29262–29270, 2018.
[61] A. Jeffrey and D. Zwillinger, *Table of Integrals, Series, and Products*, 7th ed. Amsterdam, The Netherlands: Elsevier, 2007.
[62] D. J. Maširević and T. K. Pogány, "On series representations for modified Bessel function of second kind of integer order," *Integral Transf. Special Functions*, vol. 30, no. 3, pp. 181–189, Mar. 2019.

Tan N. Nguyen (Member, IEEE) was born in Nha Trang, Vietnam, in 1986. He received the B.S. degree in electronics from the Ho Chi Minh University of Natural Sciences, Ho Chi Minh City, Vietnam, in 2008, the M.S. degree in telecommunications engineering from Vietnam National University, Ho Chi Minh City, in 2012, and the Ph.D. degree in communications technologies from the Faculty of Electrical Engineering and Computer Science, VSB—Technical University of Ostrava, Ostrava, Czech Republic, in 2019.

He joined the Faculty of Electrical and Electronics Engineering, Ton Duc Thang University, Ho Chi Minh City, in 2013, where he has been lecturing since then. His major interests are cooperative communications, cognitive radio, and physical layer security.

Dinh-Hieu Tran (Student Member, IEEE) was born in Gia Lai, Vietnam, in 1989. He received the B.E. degree from the Electronics and Telecommunication Engineering, Ho Chi Minh City University of Technology, Vietnam, in 2012 and the M.Sc. degree (Hons.), in electronics and computer engineering from Hongik University, South Korea, in 2017. He is currently pursuing the Ph.D. degree with the Interdisciplinary Centre for Security, Reliability and Trust (SnT), University of Luxembourg, under the supervision of Prof. Symeon Chatzinotas and Prof. Björn Ottersten.

He was a Research Associate with the University of Luxembourg. He is currently a Senior Research Specialist with Nokia, France. His research interests include non-terrestrial-networks, 3GPP, and B5G for wireless.

Mr. Tran received the Hongik Rector Award for his excellence during his master's study at Hongik University, in 2016. He was a co-recipient of the IS3C 2016 Best Paper Award. In 2021, he was nominated for the Best Ph.D. Thesis Award at the University of Luxembourg. In 2022, he was nominated for the FNR Outstanding Thesis Award. He won the "Excellent thesis award 2022 in Doctoral School Science and Engineering" at the University of Luxembourg, in 2022.

Trinh Van Chien (Member, IEEE) received the B.S. degree in electronics and telecommunications from the Hanoi University of Science and Technology (HUST), Hanoi, Vietnam, in 2012, the M.S. degree in electrical and computer engineering from Sungkyunkwan University (SKKU), Seoul, South Korea, in 2014, and the Ph.D. degree in communication systems from Linköping University (LiU), Linköping, Sweden, in 2020.

He was a Research Associate with the University of Luxembourg, Esch-sur-Alzette, Luxembourg. He is currently with the School of Information and Communication Technology (SoICT), HUST. His interest lies in convex optimization problems and machine learning applications for wireless communications and image & video processing.

Dr. Chien received the Award of Scientific Excellence in the first year of the 5G wireless project funded by European Union Horizon 2020. He was an IEEE Wireless Communications Letters Exemplary Reviewer in 2016, 2017, and 2021.

Van-Duc Phan was born in Vietnam in 1975. He received the M.S. degree from the Department of Electric, Electrical and Telecommunications Engineering, Ho Chi Minh City University of Transport, Ho Chi Minh City, Vietnam, and the Ph.D. degree from the Department of Mechanical and Automation Engineering, Da-Yeh University, Changhua, Taiwan.

His current research interests are sliding mode controls, nonlinear systems and active magnetic bearings, flywheel energy storage systems, power system optimization, optimization algorithms, renewable energies, energy harvesting (EH) enabled cooperative networks, optical property improvement, lighting performance of white LEDs, energy-efficient LED driver integrated circuits, novel radio access technologies, and physical security in communications networks.

Nhat-Tien Nguyen received the B.Eng. degree from the Posts and Telecommunications Institute of Technology, Ho Chi Minh City, Vietnam, and the M.Eng. degree from the Ho Chi Minh City University of Technology (HCMUT), Ho Chi Minh City, in 2017. He is currently pursuing the Ph.D. degree in communication technology with the VSB—Technical University of Ostrava, Ostrava, Czech Republic.

He was a Senior Technician with Saigon Postel Corporation, Ho Chi Minh City, in 2003. He was a Lecturer with Saigon University, Ho Chi Minh City, in 2018. His research interests include multiple-input multiple-output (MIMO), nonorthogonal multiple access (NOMA), D2D transmission, energy harvesting, millimeter-wave communications, hybrid satellite-terrestrial networks, and wireless sensor networks.

Miroslav Voznak (Senior Member, IEEE) received the Ph.D. degree in telecommunications from the Faculty of Electrical Engineering and Computer Science, VSB—Technical University of Ostrava, Ostrava, Czech Republic, in 2002, and the Habilitation degree in 2009.

He was appointed as a Full Professor of Electronics and Communications Technologies in 2017. According to the Stanford University study released in 2020, he is one of the World's Top 2% of Scientists in Networking & Telecommunications and Information & Communications Technologies. He participated in six projects funded by the EU in programs managed directly by the European Commission. He is currently a Principal Investigator in the research project QUANTUM5 funded by NATO, which focuses on the application of quantum cryptography in 5G campus networks. He has authored or coauthored over 100 articles indexed in SCI/SCIE journals. His research interests generally focus on ICT, especially the quality of service and experience, network security, wireless networks, and big data analytics.

Dr. Voznak has served as the General Chair of the 11th IFIP Wireless and Mobile Networking Conference in 2018 and the 24th IEEE/ACM International Symposium on Distributed Simulation and Real Time Applications in 2020.

Symeon Chatzinotas (Senior Member, IEEE) was a Visiting Professor with the University of Parma, Parma, Italy, lecturing on 5G wireless networks. He was involved in numerous research and development projects for NCSR Demokritos, Athens, Greece, CERTH Hellas and CCSR, and the University of Surrey, Guildford, U.K. He is currently a Full Professor/Chief Scientist I in satellite communications and the Head of the SIGCOM Research Group, Interdisciplinary Centre for Security, Reliability and Trust (SnT), University of Luxembourg, Esch-sur-Alzette, Luxembourg. He coordinates research activities in communications and networking, acting as a PI in over 20 projects, and is the main representative for 3GPP, ETSI, and DVB. He has (co)authored more than 450 technical papers in refereed international journals, conferences, and scientific books.

Dr. Chatzinotas was co-recipient of the 2014 IEEE Distinguished Contributions to Satellite Communications Award and the Best Paper Awards at EURASIP JWCN, CROWNCOM, and ICSSC. He is on the Editorial Board of the IEEE TRANSACTIONS ON COMMUNICATIONS, IEEE OPEN JOURNAL OF VEHICULAR TECHNOLOGY, and the *International Journal of Satellite Communications and Networking*.

Björn Ottersten (Fellow, IEEE) received the M.S. degree in electrical engineering and applied physics from Linköping University, Linköping, Sweden, in 1986, and the Ph.D. degree in electrical engineering from Stanford University, Stanford, CA, USA, in 1990.

He has held research positions at the Department of Electrical Engineering, Linköping University, the Information Systems Laboratory, Stanford University, the Katholieke Universiteit Leuven, Leuven, Belgium, and the University of Luxembourg, Esch-sur-Alzette, Luxembourg. From 1996 to 1997, he was the Director of Research of ArrayComm, Inc., a startup in San Jose, CA, USA, based on his patented technology. In 1991, he was appointed as a Professor of Signal Processing at the Royal Institute of Technology (KTH), Stockholm, Sweden. He has been the Head of the Department for Signals, Sensors, and Systems and the Dean of the School of Electrical Engineering, KTH. He is currently the Director of the Interdisciplinary Centre for Security, Reliability and Trust, University of Luxembourg.

Dr. Ottersten is a Fellow of EURASIP. He has been a Board Member of the IEEE Signal Processing Society and the Swedish Research Council. He was a recipient of the IEEE Signal Processing Society Technical Achievement Award, the EURASIP Group Technical Achievement Award, and the European Research Council Advanced Research Grant twice. He has coauthored journal articles that received the IEEE Signal Processing Society Best Paper Awards in 1993, 2001, 2006, 2013, and 2019, and nine IEEE Conference Papers Best Paper Awards. He serves on the boards of EURASIP and the Swedish Foundation for Strategic Research. He has served as the Editor-in-Chief of *Journal on Advances in Signal Processing* (EURASIP) and acted on the editorial boards of IEEE TRANSACTIONS ON SIGNAL PROCESSING, *IEEE Signal Processing Magazine*, IEEE OPEN JOURNAL OF SIGNAL PROCESSING, *Journal on Advances in Signal Processing* (EURASIP), and *Foundations and Trends in Signal Processing*.

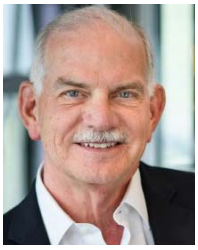

H. Vincent Poor (Life Fellow, IEEE) received the Ph.D. degree in EECS from Princeton University, Princeton, NJ, USA, in 1977.

From 1977 to 1990, he was on the faculty of the University of Illinois at Urbana–Champaign, Champaign, IL, USA. Since 1990, he has been on the faculty of Princeton University, where he is currently the Michael Henry Strater University Professor. From 2006 to 2016, he was the Dean of the School of Engineering and Applied Science, Princeton University. He has also held visiting appointments at several other universities, including most recently at the University of California at Berkeley, Berkeley, CA, USA, and the University of Cambridge, Cambridge, U.K. His research interests are in the areas of information theory, machine learning, and network science, and their applications in wireless networks, energy systems, and related fields. Among his publications in these areas is the forthcoming book *Machine Learning and Wireless Communications* (Cambridge University Press).

Dr. Poor is a member of the National Academy of Engineering and the National Academy of Sciences and a Foreign Member of the Chinese Academy of Sciences, the Royal Society, and other national and international academies. He received the IEEE Alexander Graham Bell Medal in 2017.